END
3-81

AD A094794

LEVEL · R-1979

DAVIDSON LABORATORY

Report SIT-DL-79-9-1979

September 1980

A THEORETICAL PROCEDURE
FOR CALCULATING PROPELLER-INDUCED HULL FORCES

by

S. Tsakonas and Daniel T. Valentine

APPROVED FOR PUBLIC RELEASE:
DISTRIBUTION UNLIMITED

STEVENS INSTITUTE
OF TECHNOLOGY

CASTLE POINT STATION
HOROKEN, NEW JERSEY 07030

R-1979

81 2 09 083

REPORT DOCUMENTATION PAGE	READ INSTRUCTIONS BEFORE COMPLETING FORM

1. REPORT NUMBER	2. GOVT ACCESSION NO.	3. RECIPIENT'S CATALOG NUMBER
SIT-DL-79-9-1979	AD-A094 794	

4. TITLE (and Subtitle)	5. TYPE OF REPORT & PERIOD COVERED
A THEORETICAL PROCEDURE FOR CALCULATING PROPELLER-INDUCED HULL FORCES.	FINAL
	6. PERFORMING ORG. REPORT NUMBER

7. AUTHOR(s)	8. CONTRACT OR GRANT NUMBER(s)
S. Tsakonas and Daniel T. Valentine	N00014-76-C-0862

9. PERFORMING ORGANIZATION NAME AND ADDRESS	10. PROGRAM ELEMENT, PROJECT, TASK AREA & WORK UNIT NUMBERS
Davidson Laboratory Stevens Institute of Technology Castle Point Station, Hoboken, NJ 07030	

11. CONTROLLING OFFICE NAME AND ADDRESS	12. REPORT DATE
David W. Taylor Naval Ship Research and Development Center, Code 1505 Bethesda, MD 20084	September 1980
	13. NUMBER OF PAGES
	viii + 44 pp.

14. MONITORING AGENCY NAME & ADDRESS(if different from Controlling Office)	15. SECURITY CLASS. (of this report)
Office of Naval Research 800 N. Quincy Street Arlington, VA 22217	UNCLASSIFIED
	15a. DECLASSIFICATION/DOWNGRADING SCHEDULE

16. DISTRIBUTION STATEMENT (of this Report)

APPROVED FOR PUBLIC RELEASE; DISTRIBUTION UNLIMITED

17. DISTRIBUTION STATEMENT (of the abstract entered in Block 20, if different from Report)

18. SUPPLEMENTARY NOTES

19. KEY WORDS (Continue on reverse side if necessary and identify by block number)

Propeller-Induced Hull Forces

20. ABSTRACT (Continue on reverse side if necessary and identify by block number)

A method based on rational mechanics is presented for predicting hydro-dynamic forces and moments on a hull of arbitrary geometry as a reaction to the propeller-induced velocity field. This method assumes that the hull surface can be represented by a distribution of sources. The numerical pro-cedure is adapted to the CDC 7600 or Cyber 176 digital computer which furnishes the strength of the source distribution over the hull and the vertical component of the propeller-induced hull force at blade frequency.
[Cont'd]

DD FORM 1473 EDITION OF 1 NOV 65 IS OBSOLETE
1 JAN 73
S/N 0102-014-6601

20. ABSTRACT (Cont'd)

The program is executed for two widely different cases for which experimental measurements are available: 1) a spheroidal head in the presence of a 3-bladed propeller operating in uniform inflow, and 2) a Series 60 hull model (V-form stern) driven by a 4-bladed propeller. Theoretical predictions show agreement with corresponding experimental measurements within 11% for the body of revolution and 27% for the surface ship.

A disadvantage of this approach is the excessive computing time required not only because the oscillatory nature of the propeller velocity field dictates that the hull be divided into a large number of small quadrilaterals but also because the representation of the hull surface by sources requires the evaluation of three components of the normal velocity induced by the propeller, for all possible combinations of frequencies of the loading and propagation functions.

A new method has lately been devised which replaces the sources by a distribution of doublets, thus replacing the three components of normal velocity by the negative of the velocity potential which has no directivity. Preliminary results show a substantial reduction in computing time and improvement in the accuracy of the results as well. The calculated theoretical predictions for the quadrilateral distribution now show an agreement with the measurements within 2% for the body of revolution and 10% for the surface ship.

It should be realized, however, that Lewis's measurements involved the combined effect of a force and a couple, in contrast to the theoretical prediction which gives only a vertical force. Thus, a one-to-one comparison is currently not possible.
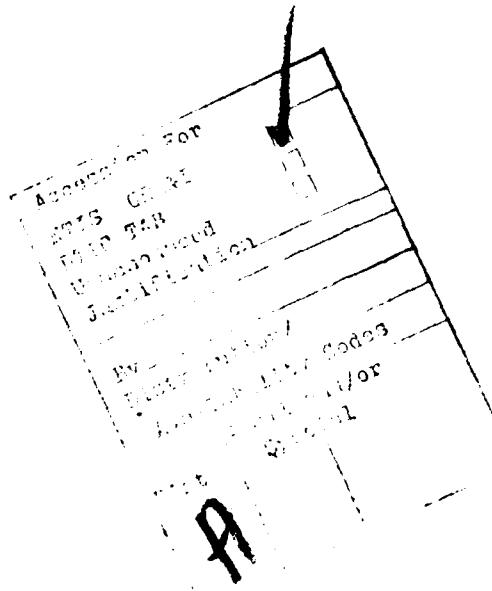
STEVENS INSTITUTE OF TECHNOLOGY

DAVIDSON LABORATORY
CASTLE POINT STATION
HOBOKEN, NEW JERSEY

Report SIT-DL-79-9-1979

September 1980

A THEORETICAL PROCEDURE
## FOR CALCULATING PROPELLER-INDUCED HULL FORCES

by

S. Tsakonas and Daniel T. Valentine

Approved:
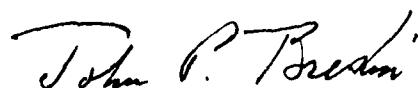
John P. Breslin

John P. Breslin
Director

vii + 44 pp.

ABSTRACT

A method based on rational mechanics is presented for predicting hydrodynamic forces and moments on a hull of arbitrary geometry as a re- action to the propeller-induced velocity field. This method assumes that the hull surface can be represented by a distribution of sources. The numerical procedure is adapted to the CDC 7600 or Cyber 176 digital com- puter which furnishes the strengths of the source distribution over the hull and the vertical component of the propeller-induced hull force at blade frequency. The program is executed for two widely different cases for which experimental measurements are available: 1) a spheroidal head in the presence of a 3-bladed propeller operating in uniform inflow, and 2) a Series 60 hull model (V-form stern) driven by a 4-bladed propeller. Theoretical predictions show agreement with corresponding experimental measure- ments within 11% for the body of revolution and 27% for the surface ship.

A disadvantage of this approach is the excessive computing time required not only because the oscillatory nature of the propeller velocity field dictates that the hull be divided into a large number of small quadrilaterals but also because the representation of the hull surface by sources requires the evaluation of three components of the normal velocity induced by the propeller, for all possible combinations of frequencies of the loading and propagation functions.

A new method has lately been devised which replaces the sources by a distribution of doublets, thus replacing the three components of normal velocity by the negative of the velocity potential which has no directiv- ity. Preliminary results show a substantial reduction in computing time and improvement in the accuracy of the results as well. The calculated theoretical predictions for the same quadrilateral distribution now show an agreement with the measurements within 2% for the body of revolution and 10% for the surface ship.

It should be realized, however, that Lewis's measurements involved the combined effect of a force and a couple, in contrast to the theo- retical prediction which gives only a vertical force. Thus, a one-to-one comparison is currently not possible.

TABLE OF CONTENTS

NOMENCLATURE

$a = \Omega/U$	angular velocity/free stream velocity
$\bar{a}$	designation of NACA-a meanline
c	expanded chord length
D	propeller diameter
F	force
f	blade thickness distribution
$I_m(\ )$	modified Bessel function of first kind, of order m
i	index
j	index
$\bar{K}(m,\bar{n})$	propagation or influence function
$\bar{K}_x, \bar{K}_\varphi, \bar{K}_r$	derivatives of propagation functions with respect to x,φ,r
$K_m(\ )$	modified Bessel function of second kind, of order m
k	variable of integration
L	loading
ℓ	integer multiple
$M(\xi,\rho,\theta_o)$	strength of source distribution on propeller blade
m	index of summation
N	number of blades
n	blade index
n	rps
$\bar{n}$	order of chordwise mode
$\hat{n}$	outward unit normal
p	pressure
Δp	pressure jump
q	order of harmonic of inflow field

R, R_1	Descartes distance
S	surface
t	time, sec
t_o	maximum thickness of blade
U	free stream velocity
u	velocity component
V	resulting velocity
V_x, V_y, V_z	velocity in x,y,z direction
X, Y, Z	rectangular coordinate system of hull
x, y, z	rectangular coordinate system of propeller
x, r, φ	cylindrical coordinates of point in space
θ_b	subtended angle of projected blade semichord
θ_α	angular chordwise location of loading point on propeller blade
$\Lambda^{(\bar{n})}(\ )$	result of chordwise (θ_α) integration for assumed chordwise mode (see Reference 5)
λ	positive integer
ξ, η, ζ	rectangular coordinates of source distribution on hull
ξ, ρ, θ_o	cylindrical coordinates of loading point on propeller
ρ_f	mass density of fluid
$\sigma(\xi, \eta, \zeta; t)$	source density on hull
σ	angular measure of skewness of propeller blade
τ	variable of integration
ϕ	total velocity potential
φ_S	diffraction potential of hull boundary
φ_P	propeller radiated potential
φ_D	diffraction potential of hull
Ψ	acceleration potential
Ω	region of source on hull (Eq.17)
Ω	magnitude of angular velocity of propeller (Eq.39)
ω	angular frequency

INTRODUCTION

One of the primary considerations of naval architects in designing propeller-stern configurations is minimization of propeller-induced hull vibration. One characteristic which determines the selection of any particular design over another is the expected level of vibratory excitations at integer multiples of blade frequency.

A method based on rational mechanics has been evolved at Davidson Laboratory for predicting the forces and moments generated on the shaft and on the hull surface for arbitrary propeller hull geometries and their given wakes. It couples computational methods for predicting unsteady propeller blade loadings, and the field point inductions due to loadings and blade thickness effects, to a computational method for the hydrodynamic reactions of a hull of specified geometry.

The forces generated by the propeller which excite ship structural vibration are composed of those generated by the fanning action of the blades on the neighboring hull and those generated on the shaft, namely, the bearing forces and moments. The surface forces depend on all shaft frequencies of the blade loading, while the blade frequency bearing forces and moments are caused by various loadings, some at the blade frequency of interest and others, one above and one below the blade frequency. The propeller operates in a spatially varying inflow of axial, radial and tangential components of velocity. Within the assumptions of linearized propeller theory, the blades respond to the variations in the axial and tangential velocities only. As the blades traverse the wake, they respond to the wake harmonics in such a manner that the thrust and torque are due to integer multiples of the blade frequency wake harmonics, and the bearing forces and moments are due to frequencies one unit above and one unit below the integer multiple of blade frequency($\ell N+1$ and $\ell N-1$ times Ω, where N is the number of blades, Ω is the shaft angular velocity, and ℓ is the multiple of interest.) These forces are the sum of those acting on each blade. However, each blade responds to all the harmonics of the circumferential variation of the wake. Each of these produce a contribution to the radiated or induced field of the propeller at integer multiples

of blade frequency. In addition, the finite thicknesses of the blades simulated by source distributions produce a blade-frequency radiation which is also accounted for in the present analysis. In the method presented here, the components of loading due to the wake and to the thickness are considered separately, and synthesized at the end. This procedure is both convenient and appropriate because the theory is linear.

The objective of the present investigation is to develop a theoretical approach to evaluate the propeller-induced vibratory hull forces. Details of the development of the mathematical models applied to the unsteady propeller/hull interaction problem are presented in this report. They are followed by descriptions of the numerical analysis procedure and the coded algorithm. The vertical hull force is calculated for two cases for which experimental data are available. The agreement obtained for these first calculations tends to substantiate the approach taken to solve the unsteady propeller/hull interaction problem; however, it is recognized that additional checking is advisable before this tool is to be applied on a regular basis. Comparisons with other cases available in the literature are in progress.

The present approach requires distribution of sources over the hull surface, the strengths of which are determined through the solution of a Fredholm integral equation of the 2nd kind in which the known function represents the propeller-induced velocity normal to the hull surface. In an investigation currently underway at Davidson Laboratory, the sources are replaced by doublets whose strength are determined by the same integral equation but with the known function replaced by the negative of the propeller velocity potential function, which has no directivity and, hence, there is only a single value at each point of the hull instead of three components of the normal velocity. This should reduce computer time considerably.

BACKGROUND

In 1965, Breslin and Eng[1]* were the first to attempt to evaluate the propeller-induced hull surface forces (i.e., the fanning forces) by combining an extended form of the Hess-Smith program[2] with a program[3] developed at Stevens Institute of Technology to calculate the propeller-induced velocity field. The latter program was based on representing the propeller blades by lifting lines and was for a propeller operating in uniform inflow having thus steady state (time invariant) blade loading only. A numerical procedure was developed for the IBM 7090 digital computer which had to be abandoned as impractical because of the excessive time required by computers of that era.

More recently, Vorus[4] developed a method which seeks to avoid solving the diffraction or scattering problem posed here by generating the hull in the presence of the nonuniform onset flow from the propeller. His method, which uses a reciprocity theorem, produces a formula for a particular hull force component in terms of integrations over the propeller blades of quantities (approximated by asymptotic expansions) induced at the blades by unit velocity motion of the hull in the plane of the desired force. Thus to determine three forces and three couples, six boundary-value problems must be solved. In contrast, the method advanced here requires the solution of only one boundary-value problem and all forces and moments are obtained by integrations. Moreover, by using the Hess-Smith program, the arbitrary hull shape is exactly taken into account whereas Vorus uses a strip theory to model the hull; strip methods tend to be inaccurate near the stern of three-dimensional bodies.

Since the first attempt to compute the unsteady propeller/hull interaction problem by Breslin and Eng,[1] systematic investigations have been undertaken to improve propeller representations and to treat more realistic operating conditions. An unsteady lifting surface theory has been developed

---

*Superior numbers in text matter refer to similarly numbered references listed at the end of this report.

3

and coded for computing the steady and unsteady propeller blade forces and moments taking into account finite chord lengths, helicoidal geometry, thickness, mutual blade interaction, and spatial nonuniformity of the inflow into the propeller disc. A detailed documentation of the computer program developed on a CDC 6600 high-speed digital computer has been issued.[5,6] The program furnishes a procedure to compute the mean (time averaged) and vibratory blade pressure distributions together with the integrated hydrodynamic forces, moments and blade bending moments about any face-pitch line. Furthermore, it provides the necessary information for the study of inception of cavitation as well as for the study of blade stress analysis which can be performed by combining the propeller program with the STARDYNE-CDC program (or the like) based on a finite element model of the blade structure.[7]

Based on the unsteady lifting surface theory of marine propellers developed at the Davidson Laboratory, theoretical methods and computer codes have been developed to compute the mean and vibratory velocity and pressure fields induced by a noncavitating propeller operating in both uniform and nonuniform inflow fields. Both loading and thickness effects have been taken into account in evaluating the propeller-induced velocity field.[8,9]

In the present investigation a form of the extended Lagally Theorem is developed and programmed to compute the propeller-induced hull forces. The velocity field program based on the unsteady lifting surface theory was exercised extensively before it was merged with the Lagally Theorem code and the Hess-Smith code to provide a self-contained computer code for calculating the propeller-induced vibratory forces. The details of this code are described in the sections to follow.

4

PROPELLER-INDUCED VIBRATORY FORCES

In this section a derivation of the extended Lagally Theorem is given which will be utilized for calculating the hull surface forces. The vector equation of motion of an incompressible inviscid fluid is taken to be:

$$\frac{\partial \underset{\sim}{u}}{\partial t} + (\underset{\sim}{u} \cdot \nabla)\underset{\sim}{u} = -\frac{1}{\rho_f} \nabla p_T \tag{1}$$

where $\underset{\sim}{u}$ is the velocity, p_T is the total pressure (including perturbation), and ρ_f the mass density.

The velocity field satisfies the continuity equation

$$\nabla \cdot \underset{\sim}{u} = 0 \tag{2}$$

and upon joining the condition of irrotationality, the total velocity field may be written in terms of a potential defined by

$$\underset{\sim}{u} = \nabla \Phi \tag{3}$$

From Eq.(2) it is observed that $\nabla^2 \Phi = 0$. Substituting Eq.(3) into Eq.(1) and integrating once yields

$$\frac{\partial \Phi}{\partial t} + \frac{1}{2} \nabla \Phi \cdot \nabla \Phi = -\frac{p_T}{\rho_f} \tag{4}$$

which is a form of the unsteady Bernoulli equation.

The total velocity potential for the flow under consideration may be written as

$$\Phi(\underset{\sim}{x},t) = U\underset{\sim}{x} + \varphi_S(\underset{\sim}{x}) + \varphi_P(\underset{\sim}{x},t) + \varphi_D(\underset{\sim}{x},t)$$

or

$$\Phi(\underset{\sim}{x},t) = U\underset{\sim}{x} + \varphi_S(\underset{\sim}{x}) + \varphi(\underset{\sim}{x},t) \tag{5}$$

where $U\underset{\sim}{x}$ is the potential of the onset flow from $\underset{\sim}{x} \to -\infty$, $\varphi_S(\underset{\sim}{x})$ is the diffraction potential of the hull boundary in response to the potential $U\underset{\sim}{x}$, $\varphi_P(\underset{\sim}{x},t)$ is the propeller radiated potential, and $\varphi_D(\underset{\sim}{x},t)$ is the diffraction potential of the hull in response to the onset flow described by $\varphi_P(\underset{\sim}{x},t)$ which is imposed by the propeller. For convenience, the unsteady

contributions to the total potential are combined into a single function $\varphi(\underset{\sim}{x},t)$. Simple harmonic time dependence will be assumed, viz.,

$$\varphi(\underset{\sim}{x},t) = \sum_{\ell=0}^{\infty} \varphi_\ell(\underset{\sim}{x}) e^{i\ell N\omega t} \tag{6}$$

in which

$$\nabla^2 \varphi_\ell = 0 \tag{7}$$

The boundary conditions at $\underset{\sim}{x} \to -\infty$ and $Z \to \pm\infty$ are given by $\nabla\varphi_\ell \to 0$. $\varphi(-\infty,t)$ is taken to be zero.

The boundary condition of the hull surface is given by

$$\hat{n} \cdot \nabla\varphi_\ell(\underset{\sim}{x}) = 0 \qquad \underset{\sim}{x} \text{ on S} \qquad \text{(see Figure 1)} \tag{8}$$

where $\hat{n}$ is taken to be the outward unit normal (into the main body of fluid). The free surface condition at Y=0 is taken to be

$$\varphi_\ell(\underset{\sim}{x}) = 0 \qquad \text{on Y=0} \tag{9}$$

On substituting Eq.(5) into Eq.(4), defining $\underset{\sim}{u}_s = U\hat{i} + \nabla\varphi_S(\underset{\sim}{x})$ [which is the total time-independent convective velocity around the hull], and linearizing, the following equation of motion for the unsteady perturbations is obtained

$$\frac{\partial\varphi}{\partial t} + \underset{\sim}{u}_s \cdot \nabla\varphi = -\frac{p}{\rho_f} \tag{10}$$

where p is the part of p_T due to φ alone.

The velocity potential $\varphi(= \varphi_P + \varphi_D)$ satisfies Laplace's equation

$$\nabla^2\varphi = \nabla^2\varphi_P = \nabla^2\varphi_D = 0$$

and the following boundary conditions

$$\varphi_P = \varphi_D = 0 \qquad \text{on Y=0 \quad (the free surface)} \tag{11a}$$

$$\frac{\partial(\varphi_P + \varphi_D)}{\partial n} = 0 \qquad \text{on S} \tag{11b}$$

where Y and S are defined in Figure 1.

The hull surface force may be found by integrating the surface pressures (Eq.10) over the hull surface and its negative reflection on the

waterplane. In index notation the components of hull forces due to the propeller imposed flow field are

$$F_i = -\rho_f \iint_S \frac{\partial(\varphi_D+\varphi_P)}{\partial t} \frac{\partial X_i}{\partial n} dS - \rho_f \iint_S \left[V_{sj} \frac{\partial}{\partial X_j}\left(\varphi_D+\varphi_P\right)\right] \frac{\partial X_i}{\partial n} dS \qquad (12)$$

where V_{sj} is the j-component of the resulting time-independent velocity (as defined previously).

In the present investigation, the body or hull surface is modeled by a distribution of sources and negative source images reflected about the (X,Z)-plane (to model the free surface as a high Froude number problem — see Figure 1). Therefore, the diffraction potential may be written as

$$\varphi_D(X,Y,Z;t) = -\iint_{S'} \sigma(\xi,\eta,\zeta;t) \left(\frac{1}{R} - \frac{1}{R_1}\right) dS' \qquad (13)$$

where $\sigma(\xi,\eta,\zeta;t)$ is the source density,

$$R = \left\{(X-\xi)^2 + (Y-\eta)^2 + (Z-\zeta)^2\right\}^{\frac{1}{2}}$$

$$R_1 = \left\{(X-\xi)^2 + (Y+\eta)^2 + (Z-\zeta)^2\right\}^{\frac{1}{2}}$$

and

$$S' \equiv S$$

The temporal part of the hull force expression (Eq.12) yields

$$F_i^{(1)} = -\rho_f \frac{\partial}{\partial t} \iint_S (\varphi_D+\varphi_P) \frac{\partial X_i}{\partial n} \bigg|_+ dS \qquad (14)$$

since t and S are independent.

Since

$$\varphi_D+\varphi_P = 0 \quad \text{on } Y=0$$

the region of integration can be extended over the waterplane area S_1. Thus

$$F_i^{(1)} = -\rho_f \frac{\partial}{\partial t} \iint_{S+S_1} (\varphi_D+\varphi_P) \frac{\partial X_i}{\partial n} \bigg|_{n=0_+} dS$$

The above form is suggestive of Green's second identity since both $\varphi_D+\varphi_P$ and X_i are harmonic functions in the inner region and

7

$$\varphi_{P_+} \text{ (on outside)} = \varphi_{P_-} \text{ (on inside)}$$

and also

$$\varphi_{D_+} = \varphi_{D_-} \qquad \text{and} \qquad n_+ = -n_-$$

Thus

$$F_i^{(1)} = +\rho_f \frac{\partial}{\partial t} \iint_{S+S_1} \frac{\partial}{\partial n} (\varphi_P + \varphi_D) \Big|_{\substack{X_i \\ n=0_-}} dS \tag{15}$$

The boundary condition given by Eq.(11b) applied on the exterior of the surface S yields

$$\frac{\partial}{\partial n} (\varphi_D + \varphi_P) \Big|_+ = 0 \tag{16}$$

Furthermore, the properties of distributions of sources on curved boundaries yield[10]

$$\frac{\partial \varphi_D}{\partial n} \Big|_+ = 2\pi\sigma - \iint_{S+S_1 -\Omega} \sigma \frac{\partial}{\partial n} \left(\frac{1}{R}\right) dS \tag{17a}$$

$$\frac{\partial \varphi_D}{\partial n} \Big|_- = -2\pi\sigma - \iint_{S+S_1 -\Omega} \sigma \frac{\partial}{\partial n} \left(\frac{1}{R}\right) dS \tag{17b}$$

where $S+S_1 -\Omega$ indicates the region excluding the location of the source at X; and $\sigma = 0$ on S_1 (waterplane).

From these relations (17a,17b)

$$\frac{\partial \varphi_D}{\partial n} \Big|_+ - \frac{\partial \varphi_D}{\partial n} \Big|_- = 4\pi\sigma$$

or

$$\frac{\partial \varphi_D}{\partial n} \Big|_- = \frac{\partial \varphi_D}{\partial n} \Big|_+ - 4\pi\sigma \tag{18}$$

Since

$$\frac{\partial \varphi_P}{\partial n} \Big|_- = \frac{\partial \varphi_P}{\partial n} \Big|_+$$

Eq.(18) can be written as

$$\frac{\partial (\varphi_D + \varphi_P)}{\partial n} \Big|_- = \frac{\partial (\varphi_D + \varphi_P)}{\partial n} \Big|_+ - 4\pi\sigma$$

8

which upon substitution into Eq.(15) yields

$$F_i = -4\pi\rho_f \frac{\partial}{\partial t} \iint_S \sigma X_i \, dS + \rho_f \frac{\partial}{\partial t} \iint_{S_1} \frac{\partial}{\partial n} (\varphi_D + \varphi_P) \Big|_+ \, dS \qquad (19)$$

Here use was made of the fact that

$$X_i = 0 \quad \text{on waterplane} \quad Y = 0$$

and

$$\frac{\partial}{\partial n} (\varphi_D + \varphi_P) \Big|_+ = 0 \quad \text{on S (wetted surface)}$$

In addition, on the waterplane surface $Y = 0$

$$\frac{\partial}{\partial n} \Big|_- = - \frac{\partial}{\partial Y}$$

and hence

$$\frac{\partial}{\partial n} (\varphi_D + \varphi_P) \Big|_- = - \frac{\partial}{\partial Y} (\varphi_D + \varphi_P)$$

Thus Eq.(19) giving the force component F_i becomes

$$F_i = -4\pi\rho_f \frac{\partial}{\partial t} \iint_S \sigma X_i \, dS - \rho_f \frac{\partial}{\partial t} \iint_{S_1} X_i \frac{\partial}{\partial Y} (\varphi_D + \varphi_P) \Big|_{Y=0} \, dS \qquad (20)$$

It should be noted that the second term on the right-hand side of Eq.(20) is zero for the vertical force since $X_2 = Y = 0$ on S_1. Consequently, when there is a free surface this term is present only if the transverse and longitudinal forces are required. Calculations have shown that the primary contribution to the total unsteady surface force is the temporal part given by Eq.(20). The convective term described next may be neglected as was found by Vorus,[4] and by the present numerical calculations.

The convective term of the extended Lagally Theorem is given by

$$F_i^{(2)} = -\rho_f \iint_S \left[V_{s_j} \frac{\partial}{\partial X_j} (\varphi_D + \varphi_P) \right] \frac{\partial X_i}{\partial n} \, dS \qquad (21)$$

which is the second term in Eq.(12). In steady-state, propeller/hull interaction problems, the convective term described by Eq.(21) is the only contribution to the surface force on the hull. Modeling the hull by a similar type of surface distribution of singularities given by Eq.(13),

9

Cox, et.al.,[11] demonstrated that the convective term can be expressed as

$$F_i^{(2)} = -4\pi\rho_f \iint_S U_{Pi}\, \sigma_0 dS + \rho_f \iint_{S_1} \frac{\partial\varphi_S}{\partial X_i} \frac{\partial(\varphi_D + \varphi_P)}{\partial Y} dS_1 \qquad (22)$$

where σ_0 = the steady state source strength distribution

and U_{Pi} = propeller-induced velocity in the i-direction at any point on the hull surface

(See Appendix A of Reference 11.)

Consequently, the total force on the body is given by the extended Lagally Theorem as

$$F_i = F_i^{(1)} + F_i^{(2)} \qquad (23)$$

If harmonic time dependence is assumed, then for the unsteady hull force, Eq.(23) is written as

$$\hat{F}_i^{(\ell N)} = -4\pi\rho_f(i\,\ell N\omega) \iint_S \hat{\sigma}\, X_i dS - 4\pi\rho_f \iint_S \hat{U}_{Pi}\, \sigma_0 dS$$

$$-\rho_f \iint_{S_1} \left[i\,\ell N\omega X_i + \frac{\partial\varphi_S}{\partial X_i} \right] \frac{\partial(\hat{\varphi}_D + \hat{\varphi}_P)}{\partial Y} \Bigg|_{Y=0} dS \qquad (24)$$

where the circumflex ^ marks the part of any quantity q which is time dependent, i.e., setting

$$q(X,Y,Z;t) = \hat{q}(X,Y,Z)e^{i\,\ell N\omega t}$$

The frequency selected is the frequency at which the propeller velocity field is radiated. It is Eq.(24) which is programmed to compute the hull surface forces according to the procedure developed in this study.

POTENTIAL FLOW ABOUT THE SHIP HULL

The problem considered in this section is that of the flow of an ideal, inviscid fluid about an arbitrarily shaped, three-dimensional ship hull modeled by a surface distribution of sources. The method developed and programmed by Hess and Smith[2] is employed to solve the Fredholm integral equation of the second kind generated by the condition that the hull is a stream surface. The source distribution is discretized into plane quadrilateral elements of constant density and the simultaneous algebraic equations resulting from the discretization of the integral equations are solved by a Gauss-Seidel iteration scheme. The numerical analysis procedure and theoretical model employed by Hess and Smith are adequately described in Reference 2. A synopsis of the theory and the resulting boundary-value problem is given below:

The ship hull surface denoted by S is given, in Cartesian coordinates, by the equation

$$F(X,Y,Z) = 0 \tag{25}$$

where X,Y,Z are defined in Figure 1. The hull is subjected to the free stream and the propeller-induced velocity fields. The steady-state propeller inductions are ignored in the present investigation; only the unsteady (blade frequency) hull surface forces are sought of which the convective contribution can be shown to be small. The propeller-induced, blade frequency velocity field is expressed in complex form (as described in the next section) and has cosine (real) and sine (imaginary) components. The real and imaginary inductions are considered separately as two input flows in the Hess-Smith method. Therefore, the three onset flows about the ship hull which are considered as input to the Hess-Smith computer code are: (a) A uniform onset flow $\underset{\sim}{V}_\infty = U\hat{i}$, (b) Real part of the propeller-induced velocity field $\underset{\sim}{V}_P^R$, (c) Imaginary part of the propeller-induced velocity field, $\underset{\sim}{V}_P^i$.

The Hess-Smith potential satisfies

$$\nabla^2 \Psi_{HS} = 0 \tag{26}$$

on the region exterior to S which is the hull boundary plus its image. In

addition,

$$\frac{\partial \Phi}{\partial n} = 0 \qquad \text{on S} \tag{27}$$

where $\hat{n}$ is the outward directed normal to the hull pointing into the fluid outside the ship hull. If a free surface exists (denoted S_1), then the X,Z,-plane is taken to be the waterplane. It is then considered to be a plane of geometric symmetry with a Dirichlet or a Neumann boundary condition specified on the free surface if either a high Froude number or a low Froude number approximation, respectively, is desired.

The total potential for steady motion may be expressed by

$$\Phi_{HS} = UX + \varphi_S(X,Y,Z) \tag{28}$$

where φ_S is the response of the hull to UX flow. It satisfies

$$\nabla^2 \varphi_S = 0 \tag{29}$$

exterior to S, and

$$\frac{\partial \varphi_S}{\partial n} = -\hat{n} \cdot (U\hat{i}) \qquad \text{on S} \tag{30}$$

where $\hat{n} = \pm [\nabla F / |\nabla F|]_{F=0}$. The sign of $\hat{n}$ is such that it points into the fluid exterior to S. Also, it is required that

$$\varphi_S \to 0 \qquad \text{as} \quad X^2 + Y^2 + Z^2 \to \infty \tag{31}$$

For a surface distribution of sources, the diffraction potential is given by

$$\varphi_S(X,Y,Z) = - \iint_S \frac{\sigma(\xi,\eta,\zeta)}{R} \, dS \tag{32}$$

where $R = \{(X-\xi)^2 + (Y-\eta)^2 + (Z-\zeta)^2\}^{\frac{1}{2}}$ and S includes the image surface. The form of φ_S in Eq.(32) automatically satisfies Eqs.(29) and (31) for any function σ. In addition, the function σ must be determined so that the potential φ_S satisfies the boundary condition on S given by Eq.(30). It should be noted that the surface S is made up of the wetted surface and that of the image system (positive geometric image) of the hull, so that a closed body in an infinite fluid is generated, a situation which has been

12

shown[11] to be sufficient for the evaluation of the vertical force. Applying Eq.(30) requires the evaluation of the normal derivative of Eq.(32) at a point (X,Y,Z) on S. As the surface S is approached, the derivative of the integral becomes singular and its principal part must be extracted (see Kellogg[10]). This manipulation leads to the following integral equation for the surface source density distribution:

$$-\hat{n} \cdot \hat{Ui} = 2\pi\sigma(P) - \iint_S \sigma(Q) \frac{\partial}{\partial n} \frac{1}{R(P,Q)} \, dS \tag{33}$$

where σ is the source density, $\hat{n}$ is the normal vector at P, and R is the Descartes distance between P (control point) and Q (loading point). This equation is a Fredholm integral equation of the second kind for the unknown source densities σ, which are determined for the known onset flow on the hull surface specified on the left-hand side. The velocity $\hat{Ui}$ is the velocity at P due to the undisturbed stream at upstream infinity. Any flow field imposed on the locus of the hull (in the absence of the hull) may be considered. Here two other fields are considered, namely, the two components, real and imaginary, of the velocity field induced by the propeller. For each given onset flow, the source densities are computed by solving Eq.(33).

In the present investigation the coded numerical procedure developed by Hess and Smith[2] is applied to solve Eq.(33). The three onset flows considered produce three source densities, namely, σ_o due to the uniform steady motion of the hull and its positive image moving in an infinite fluid, σ_R due to the real part of the propeller-induced onset flow, and σ_I due to the imaginary part of the propeller-induced onset flow. The blade frequency radiated velocities induced by the propeller are the velocities imposed here.

VELOCITY FIELD INDUCED BY THE PROPELLER

Considerable effort has been devoted to the development of unsteady
lifting surface theory for propellers operating in a spatially nonuniform
hull wake. The theoretical analysis and numerical techniques developed at
Davidson Laboratory are based on modeling the propeller blades with sources
and pressure dipole singularities. The computer code permits the calcula-
tion of unsteady blade pressure distributions, forces, and moments for a
given propeller geometry — number of blades, pitch, chordlength, camber,
thickness, skew, and rake — and a given inflow field. Details of the
theory, analysis and computer program have been reported elsewhere (see
Tsakonas, et.al.[5,6]). The theory has been extended to compute the field
point velocities.[8,9] Both the loading and velocity field programs[12] have
been incorporated into the propeller/hull interaction computer code des-
cribed here. The steady and unsteady blade loadings and their concomitant
field point inductions are the responses of the propeller blades to the hull
wake.

The hull wake longitudinal and tangential components as measured in
the propeller plane are resolved by Fourier analysis into a circumferential
mean component and higher harmonics in shaft rotation frequency. The higher
harmonics which are oscillatory in time with respect to the propeller give
rise to unsteady loadings on the blade in a manner analogous to an airfoil
encountering a sinusoidal gust. Within the linear approximation, each pro-
duces a component of unsteady blade loading at the corresponding frequency.
Upon summing over all the blades, only certain harmonics contribute to the
net exciting forces and moments acting on the shaft, namely, ℓN for the
thrust and torque and $\ell N \pm 1$ for the side bearing, forces and bending moment,
where ℓ is any integer and N is the number of blades. However, all the
harmonics of loading contribute to the forces on an individual blade and
to the blade rate(and integer multiples thereof) of radiated velocity and
radiated pressure fields of the propeller (e.g., at points on the hull
surface).

A brief description of the propeller theory applied to compute the field
point velocities (which includes the velocities induced by the blade thickness
modeled by source singularities) is presented next; for further details the reader

may review References 5, 6, 8, and 9. The loading program developed at the Davidson Laboratory is called PPEXACT. Prior to calculating the hull vibratory surface forces due to the propeller by exercising the propeller/hull interaction program PIHF, the program PPEXACT (or the like) must be exercised to determine the blade loadings for all frequencies up to one plus the blade frequency, and also to determine the unsteady shaft forces and moments. The blade frequency hull forces are computed by PIHF which uses the blade loadings as input to compute first the velocity field produced by the propeller. The algorithm in the PIHF code, which utilizes the field point velocity program, the Hess-Smith program and the extended Lagally Theorem code, is described in the next section.

The propeller theoretical analysis uses the acceleration potential method to formulate a linearized, unsteady lifting-surface theory for a marine propeller operating in a spatially varying, unidirectional mean flow which is aligned with the shaft axis. Potential flow of an ideal, inviscid, incompressible, homogeneous fluid is assumed. The steady forces and moments produced by a propeller operating in a real fluid are due primarily to potential flow effects; however, since the viscous drag is significant in predicting steady performance, it is accounted for approximately in the PPEXACT program. The unsteady forces and moments are considered to be inviscid in nature. The vorticity in the oncoming flow is ignored; however, the variations in the inflow velocity are considered parametrically as is usually done in theories for marine propellers. The blades are assumed to lie on helicoidal surfaces. Therefore, the linearized equation of motion for unsteady flow, referred to a nonrotating (fixed) cylindrical coordinate system (x, r, φ) centered at the propeller axis (see Figure 2) may be written as

$$\frac{\partial \phi}{\partial t} + U \frac{\partial \phi}{\partial x} = -\frac{p}{\rho_f} = \psi \tag{34}$$

where ψ is the so-called acceleration potential and p is the local perturbation pressure. Hence,

$$\nabla^2 p = 0 \tag{35a}$$

$$p \to 0 \qquad \text{as} \quad x \to \pm \infty \tag{35b}$$

The solution to Eq.(34) subject to (35b) can be shown to be

$$\phi(x, y, z; t) = -\frac{1}{\rho_f U} \int_{-\infty}^{x} p\left(\tau, y, z; t + \frac{\tau - x}{U}\right) d\tau \tag{36}$$

15

where p is the disturbance pressure due to the propeller loading, and $\Phi(-\infty,y,z)=0$ was used.

The propeller blades are modeled by pressure dipoles (as far as their loading is concerned), and the corresponding pressure field is given by

$$p = -\frac{1}{4\pi} \iint\limits_{S} \Delta p \frac{\partial}{\partial n} \left(\frac{1}{R}\right) dS \tag{37}$$

After an harmonic analysis of Δp, Equation (37) may be written as

$$p = -\frac{1}{4\pi} \iint\limits_{S} \sum_{\lambda=0}^{\infty} \Delta P^{(\lambda)}(\xi,\rho,\theta) e^{i\lambda\Omega t} \frac{\partial}{\partial n}\left(\frac{1}{R}\right) dS \tag{38}$$

where R is the Descartes distance between the control point (x,r,φ) (i.e., fixed point in space) and the loading point (ξ,ρ,θ) rotating with angular velocity $-\Omega$ and lying on a helicoidal surface.

Equations (36) and (38) are combined and summed over the number of blades to yield the equation for the velocity potential at a point (x,r,φ) due to the blade loading of an N-bladed propeller, namely,

$$\Phi(x,r,\varphi;q)= +\frac{1}{4\pi\rho_f U} \sum_{n=1}^{N} \iint\limits_{S} \sum_{\lambda=0}^{\infty} \Delta P^{(\lambda)}(\xi,\rho,\theta_o) e^{i\lambda(\Omega t - \bar{\theta}_n)}$$

$$\cdot \int_{-\infty}^{x} e^{i\lambda a(\tau-x)} \frac{\partial}{\partial n}\left(\frac{1}{R}\right) d\tau dS \tag{39}$$

where q and λ are positive integers defining the desired frequency of the velocity field and the appropriate frequency of the propeller loading, respectively. Note that $q=0$ corresponds to the steady-state velocity field, and $q=N$ corresponds to the blade frequency induced velocity field. The latter is of interest here. The other parameters are defined as follows:

x,r,φ = cylindrical coordinates of point in space referred to axes with origin at the propeller hub

ξ,ρ,θ_o = cylindrical coordinates of loading point on propeller

U = free stream velocity, fps

ρ_f = fluid density, slugs/cu ft

$-\Omega$ = angular velocity of the propeller, rad/sec

a = Ω/U, 1/ft

$\Delta P^{(\lambda)}(\xi,\rho,\theta_o)$ = propeller loading, or pressure jump across the propeller blade, psf

16

$$R = \{(\tau-\xi)^2 + r^2 + \rho^2 - 2r\rho \cos[\theta_o - \Omega t + \bar{\theta}_n - a(\tau-x) - \varphi]\}^{\frac{1}{2}}, \text{ ft}$$

$\dfrac{\partial}{\partial n}$ = normal derivative on the helicoidal surface at the loading point (ξ, ρ, θ_o) on the propeller

$$\bar{\theta}_n = \frac{2\pi}{N}(n-1) \qquad n = 1, 2, \dots N$$

S = blade surface, sq ft

The normal derivative to the helicoidal surface (specified by $\xi = \theta_o/a$) is

$$\frac{\partial}{\partial n} = \frac{\rho}{(1 + a^2\rho^2)^{\frac{1}{2}}} \left(a \frac{\partial}{\partial \xi} - \frac{1}{\rho^2} \frac{\partial}{\partial \theta_o}\right)$$

Use is made of the following:

a) <u>Expansion scheme for the reciprocal of the Descartes distance R</u>

$$\frac{1}{R} = \frac{1}{\pi} \sum_{m=-\infty}^{\infty} e^{im(\theta_o - \Omega t + \bar{\theta}_n - a(\tau-x) - \varphi)} \cdot \int_{-\infty}^{\infty} I_m(|k|\rho) K_m(|k|r) e^{i(\tau-\xi)k} dk$$

(when $\rho < r$, otherewise ρ and r are interchanged in the modified Bessel functions).

b) <u>Summation over the propeller blades</u>

$$\sum_{n=1}^{N} e^{-i(\lambda-m)\bar{\theta}_n} = \begin{cases} N & \text{when } \lambda-m = \ell N, \ \ell = 0, \pm 1, \pm 2, \dots \\ 0 & \text{when } \lambda-m \neq \ell N \end{cases}$$

and from the time-dependent factor

$$\lambda - m = q = \ell N$$

c) <u>Transformations</u>

$$L^{(\lambda)}(\rho, \theta_\alpha) = \Delta P^{(\lambda)}(\xi, \rho, \theta_o) \cdot \rho\theta_b, \text{ lb/ft}$$

where θ_b is the projected semichord at each spanwise location ρ, in radians.

$$\theta_o = \sigma - \theta_b \cos \theta_\alpha = a\xi$$

where σ is angular position of the midchord line of the projected blade from the generator line through the hub, or skewness, and θ_α is angular chordwise location of the loading point.

d) Approximation of the loading function $L^{(\lambda)}(\rho,\theta_\alpha)$ in the chordwise direction by $\bar{n}$ modes whose selection is dictated by the pressure distribution on a foil in two-dimensional flow

The velocity potential can then be written as

$$\Phi(x,r,\varphi;q) = \int_\rho \sum_{\bar{n}=1}^\infty \sum_{\lambda=0}^\infty L^{(\lambda,\bar{n})}(\rho) e^{iq\Omega t} \bar{K}^{(m,\bar{n})} d\rho \qquad (40)$$

where the function $\bar{K}^{(m,\bar{n})}$, which is known as the propagation or influence function, is given by

$$\bar{K}^{(m,\bar{n})} = -\frac{iNe^{im(\sigma-\varphi)}}{4\pi\rho_f Ua} \left\{ e^{i\ell N(\sigma-ax)} \left(\frac{m}{\rho^2} - a^2\ell N\right) \right.$$

$$\cdot I_m(a|\ell N|\rho) K_m(a|\ell N|r) \Lambda^{(\bar{n})}(\lambda\theta_b) - \frac{i}{\pi}\int_{-\infty}^\infty e^{ik(x-\sigma/a)}$$

$$\cdot \frac{(m/\rho^2+ak)}{k+a\ell N} I_m(|k|\rho) K_m(|k|r) \cdot \Lambda^{(\bar{n})} \left[\left(m-\frac{k}{a}\right)\theta_b\right] dk \right\} \qquad (41)$$

for $\rho < r$ (for $\rho > r$, ρ and r are interchanged in the modified Bessel functions). The symbol $\Lambda^{(\bar{n})}(x)$ denotes the results of the chordwise (θ_α) integration which differs with the assumed chordwise modes.

The following chordwise mode shapes have been used to model blade pressure distributions when $\lambda=0$:

(a) The so-called "roof-top" mode appropriate to NACA-$\bar{a}$-meanline cross-sections when the propeller operates at the design advance ratio. The chordwise loading is constant from $x/c = 0$ at the leading edge to $x/c = \bar{a}$ and then decreases linearly to zero at $x/c = 1$, the trailing edge.

(b) The first term of the Birnbaum series (the cotan $\theta_\alpha/2$ term) for the additional loading due to difference between off-design and design advance ratio when the propeller operates at off-design conditions.

(c) The complete Birnbaum series when the design operating conditions are not known.

When $\lambda\neq0$, the blade loading distribution is represented by the complete Birnbaum series.

The velocities in the x, y, and z directions of the Cartesian co-ordinate system with origin at the propeller center at a point x, r, φ due to the propeller operating in spatially varying inflow will be given by the appropriate components of the gradient of the velocity potential Φ.

The axial component in nondimensional form is

$$\frac{V_x}{U} = \frac{\Phi_x}{U}$$

and the y and z components are derived from

$$\frac{V_y}{U} = \frac{\Phi_y}{U} = -\frac{\Phi_r}{U} \sin\varphi - \frac{1}{r}\frac{\Phi_\varphi}{U} \cos\varphi$$

$$\frac{V_z}{U} = \frac{\Phi_z}{U} = \frac{\Phi_r}{U} \cos\varphi - \frac{1}{r}\frac{\Phi_\varphi}{U} \sin\varphi$$

Reference 8 shows that for the unsteady blade-frequency case, $q=N$, $|\ell| = 1$, which is of interest in the present study,

$$\frac{V_x^{(N)}}{U} = \frac{\Phi_x^{(N)}}{U} = \int_\rho \sum_{\bar{n}=1}^{\bar{n}\max} \sum_{\lambda=0}^{\infty} \left\{ L^{(\lambda,\bar{n})}(\rho)\bar{K}_x^{(\lambda-N,\bar{n})} \right.$$
$$\left. + \text{conj.}\left[L^{(\lambda,\bar{n})}(\rho)\bar{K}_x^{(\lambda+N,\bar{n})} \right] \right\} d\rho$$

$$\frac{V_r^{(N)}}{U} = \frac{\Phi_r^{(N)}}{U} = \int_\rho \sum_{\bar{n}=1}^{\bar{n}\max} \sum_{\lambda=0}^{\infty} \left\{ L^{(\lambda,\bar{n})}(\rho)\bar{K}_r^{(\lambda-N,\bar{n})} \right.$$
$$\left. + \text{conj.}\left[L^{(\lambda,\bar{n})}(\rho)\bar{K}_r^{(\lambda+N,\bar{n})} \right] \right\} d\rho$$

$$\frac{V_\varphi^{(N)}}{U} = \frac{\Phi_\varphi^{(N)}}{r r_0 U} = \frac{1}{r} \int_\rho \sum_{\bar{n}=1}^{\bar{n}\max} \sum_{\lambda=0}^{\infty} \left\{ L^{(\lambda,\bar{n})}(\rho)\bar{K}_\varphi^{(\lambda-N,\bar{n})} \right.$$
$$\left. + \text{conj.}\left[L^{(\lambda,\bar{n})}(\rho)\bar{K}_\varphi^{(\lambda+N,\bar{n})} \right] \right\} d\rho \qquad (42)$$

The propeller-induced velocity field is thus made up of a large number of combinations of the frequency constituents of the loading function with those of the propagation function.

The loading functions $L^{(\lambda,\bar{n})}(\rho)$ are determined through the PPEXACT program which solves the integral equation relating the unknown blade loading distribution with the known onset flow normal to the blade surfaces.[5] The derivatives of the propagation functions $\bar{K}^{(m,\bar{n})}$ present a complex problem. Beside their oscillatory character in terms of the spatial ordinates which presents the problem of selecting the proper spacing or mesh size, there is the problem of truncation of the range of integration.

In deriving the velocity potential at a field point x,r,φ due to blade thickness of an N-bladed propeller, the thickness distribution of a blade section is represented by a source-sink distribution smeared over the blade section chord. This velocity potential[9] is given by

$$\Phi_T(x,r,\varphi;t) = -\frac{1}{4\pi} \sum_{n=1}^{N} \int_{-\theta_b^\rho}^{\theta_b^\rho} \int_{\rho}^{\rho} \frac{M(\xi,\rho,\theta_o)}{R_T} \frac{\sqrt{1+a^2\rho^2}}{a\rho} \rho\,d\rho\,d\theta_o \qquad (43)$$

The source strength $M(\xi,\rho,\theta_o)$ is determined in accordance with the "thin body" approach as

$$M(\xi,\rho,\theta_o) = 2U \frac{\partial f(\xi,\rho,\theta_o)}{\partial \xi}$$

where $f(\xi,\rho,\theta_o)$ is the thickness distribution over the blade section at the radial distance ρ . The Descartes distance from a point on the propeller to the field point is

$$R_T = \left\{ (x-\xi)^2 + r^2 + \rho^2 - 2r\rho \cos(\theta_o-\Omega t-\varphi+\bar{\theta}_n) \right\}^{\frac{1}{2}}$$

It is known that the detailed geometry of the blade has little or no effect on the velocity or pressure field around an operating propeller. This is in contrast to the case of the pressure distribution on the propeller blades, where accurate and detailed information about the propeller blade section geometry including the thickness distribution is important.

Assuming that the blade section is bounded by two circular arcs which is equivalent to saying that the section is of the lenticular form, then the thickness distribution can well be represented by

$$f(\rho, \theta_\alpha) = \frac{t(\rho)}{2} \sin^2 \theta_\alpha$$

$$= \frac{t_o(\rho)}{c(\rho)} \frac{\theta_b^\rho}{a} \sqrt{1 + a^2 \rho^2} \; \sin^2 \theta_\alpha$$

where $t(\rho)$ is the maximum thickness and t_o/c the maximum thickness ratio to expanded chord.

Utilizing the expression for the thickness distribution together with the known expansion of the reciprocal of the Descartes distance, the velocity potential for the propeller blade thickness becomes[9]

$$\Phi_T(x, r, \varphi; t) = -\frac{i2aNU}{\pi^2} \sum_{\ell=-\infty}^{\infty} e^{-i\ell N(\varphi + \Omega t)} \int_\rho \frac{(1 + a^2 \rho^2)}{\theta_b^\rho} \frac{t_o(\rho)}{c(\rho)} e^{i\ell N \sigma^\rho}$$

$$\cdot \int_{-\infty}^{\infty} I_{\ell N}(|k|\rho) K_{\ell N}(|k|r) e^{ik(x - \sigma^\rho/a)}$$

$$\cdot \frac{\{\sin[(k-a\ell N)\theta_b^\rho/a] - (k-a\ell N)(\theta_b^\rho/a)\cos[(k-a\ell N)\theta_b^\rho/a]\}dkd\rho}{(k-a\ell N)^2} \tag{44}$$

The velocity components along the axes of the Cartesian coordinate system due to thickness can be determined by taking the appropriate derivatives and these velocities are then combined with those due to the loading to obtain the total propeller-induced velocity field.

A computer program adapted to a CDC 6600 or 7600, or Cyber 176 high-speed digital computer has been developed for the evaluation of the propeller-induced velocity field.

The analyses of References 8 and 9 and the corresponding computer program have been modified to furnish the contribution of the propeller image system to this velocity field at high Froude number. The use of the negative of the propeller potential located at the reflected position above the free surface satisfies the high Froude number condition on that surface. For points on the free surface this condition yields zero perturbation pressure or equivalently doubles the vertical component of the velocity induced by the direct propeller. The computer program automatically gives the propeller-induced velocity field generated from the direct and image systems together or separately, when the high Froude number condition on the free surface is to

21

be satisfied.

The program requires the coordinates of the field points to be given in cylindrical coordinates x, r, φ:

a) <u>For the direct system</u>

$$x_D = x$$

$$r_D = \sqrt{y^2 + z^2}$$

$$\varphi_D = \tan^{-1}\left(\frac{-y}{z}\right)$$

where the angular ordinate φ_D is measured in the counter-clockwise direction from the vertical (12 o'clock) position looking forward, and x, y, z are the rectangular coordinates of the axes fixed in the propeller.

b) <u>For the image system</u>

$$x_I = x$$

$$r_I = \sqrt{y^2 + (2d-z)^2}$$

$$\varphi_I = \tan^{-1}\left(\frac{-y}{2d-z}\right)$$

and φ_I is measured clockwise from the 6 o'clock position looking forward; d = distance of the propeller axis from the free surface.

The resolutions in the y and z directions are given as follows:

a) <u>For the direct system</u>

$$-\frac{V_{y_D}}{U} = \frac{V_{r_D}}{U} \sin\varphi_D + \frac{V_{\varphi_D}}{U} \cos\varphi_D$$

$$\frac{V_{z_D}}{U} = \frac{V_{r_D}}{U} \cos\varphi_D - \frac{V_{\varphi_D}}{U} \sin\varphi_D$$

b) <u>For the image system</u>

$$-\frac{V_{y_I}}{U} = \frac{V_{r_I}}{U} \sin\varphi_I + \frac{V_{\varphi_I}}{U} \cos\varphi_I$$

$$\frac{V_{z_I}}{U} = -\frac{V_{z_I}}{U} \cos\varphi_I + \frac{V_{\varphi_I}}{U} \sin\varphi_I$$

22

In the present problem, the blade frequency velocities due to the propeller and its image are computed at selected hull points where their contributions are considered to be significant. The velocities imposed by the propellers on the hull in the vicinity of the propellers are computed first. Then the range of computed points is extended until it is observed that the additions to the force are negligible from the most distant panels considered. All the quadrilateral elements representing the hull that are outside the direct range of propeller influence can therefore be set to zero.

The real and imaginary parts of the propeller-induced velocities calculated by the procedure described above yield the two sets of boundary conditions ("real" and "imaginary" onset flows) applied to the ship by input to the Hess-Smith program, which is part of PIHF.

Vorus[4] has noted that the calculation of just the vertical force can be accomplished by treating the hull and its image as a completely submerged body in the presence of the propeller alone, this being equivalent to the force generated on the wetted portion of the hull in the presence of both its geometric image (containing sources of opposite sign) and the propeller plus its negative image. As this observation obviates the need for the inductions from the image propeller, we have calculated the vertical force as though the body were completely submerged in the presence of only the propeller. The first term of Eq.(12) applies with S representing the double body surface.

CORRELATION OF THEORY WITH EXPERIMENTS

By combining programs for computing the unsteady blade loadings and the field point inductions with a program for the evaluation of hydrodynamic reactions of a hull to those inductions, a theoretical procedure has been developed and a new program has been established and adapted to a CDC-6600 series or Cyber 176 high-speed digital computer which furnishes (a) the propeller-induced velocities at points on a given hull, (b) the hydrodynamic reactions of the hull to those inductions, and (c) the unsteady forces generated on the hull through the bearings and the hull plating (by the fanning action of the blades). The accuracy and usefulness of the computational procedure is investigated below by comparing theoretical predictions with experimental measurements obtained in two widely different cases.

The first set of model data was provided by measurements made at DWT Naval Ship Research & Development Center on a fully submerged spheroidal head form cantilevered from a force balance as illustrated schematically in Figure 2. The force measurements were made with a three-bladed propeller NSRDC-4118 located 16 inches aft of the nose of the body with a nominal tip clearance of 3 inches operating at advance ratio J = 0.833 (design speed).

The second case selected was a Series 60 hull model (V-stern) driven by the four-bladed propeller NSRDC 3379 which was tested by the late Professor Emeritus F.M. Lewis at MIT.[13] A schematic arrangement of the propeller-hull configuration and the coordinate axis system are presented in Figure 1.

To carry out the numerical solution of the Fredholm integral equation of the second kind given by Eq.(33), the hull surfaces are subdivided into quadrilateral elements as shown in Figures 3 and 4. The quadrilateral size is crucial in calculating the hydrodynamic forces and moments, but it is rather difficult to select the proper dimensions. These are dictated by the propeller-induced velocity which is of oscillatory character as shown in Fig.5. The patch dimensions should be selected so as to fit four quadrilaterals into one cycle of spatial oscillation wherever such variations are present.

It has been suggested by Dr. Breslin that rather than calculate the propeller-induced velocity components in advance, an approximate idea of the periods of oscillation could be obtained from the exponential factors

exp(iℓNax) and exp(i$(\lambda-\ell N)\varphi$). Then for fixed radial clearance and angular position φ, the longitudinal spacing in the neighborhood of the propeller would be governed by Nax=$2\pi/4$ or x=$2\pi/4$Na . For fixed longitudinal position the transverse spacing would be governed by $|\lambda-\ell N|\varphi=2\pi/4$ which for ℓ=1 and λ=0 (uniform flow) yields φ = $2\pi/4$N.

In the case of the body of revolution the mesh size should be governed by x~0.14 propeller radius and φ~ 0.5 so that the quadrilateral sizes selected (see Fig.3) are adequate. In the case of the surface ship the longitudinal spacing should be x~0.08 propeller radius and the transverse spacing governed by φ~0.4. The longitudinal spacing shown in Figure 4 is inadequate but the transverse spacing may be considered sufficient. To impose the required longitudinal spacing would increase the already large number of quadrilaterals considerably and, hence, the number of field points at which the three velocity components are to be evaluated with all the combinations of the frequencies of the loading and the propagation functions. This is impractical.

A study has been initiated at Davidson Laboratory to replace the present method, which represents the hull by a source distribution and requires computation of three velocity components at each field point, by a procedure which represents the hull by a doublet distribution and requires the computation of only one function, the propeller velocity potential. This method permits decreasing the mesh size of the quadrilaterals and increasing the number while still reducing computer time, and is showing considerable improvement. However, for this report the calculations have been performed using the quadrilateral arrangements shown in Figures 3 and 4.

CASE 1 — The surface of the spheroidal body is divided into 154 quadrilaterals with mesh size increasing with distance from the propeller. Each of these elements (see Figure 3) is a uniform source patch. Panels 93 through 100 were used to close the body. The geometry of these elements, together with the normal velocity (due to loading and blade thickness) induced by the propeller operating in uniform inflow, form the input to the generalized Hess-Smith program which inverts the integral equation (similar to Eq.33) and evaluates the source densities on each of the panels.

The particulars of the propeller are given in Table 1 and other characteristics are given in Table 2.

TABLE 1

PARTICULARS OF PROPELLER 4118

Propeller Designation	NSRDC 4118
Number of Blades	3
EAR	0.6
P/D at 0.7	1.08
Diameter, D, ft	1
RPM	900
Fluid Speed, U, ft/sec	12.5
Advance Ratio, J = U/nD	0.833

TABLE 2

CHARACTERISTICS OF PROPELLER 4118

z/z_o	Maximum camber/chord m_x/c	Maximum thickness/chord t_o/c	Ratio of leading-edge radius to chord ρ_o
0.25	0.0228	0.090	0.00525
0.35	0.0231	0.068	0.00290
0.45	0.0224	0.052	0.00170
0.55	0.0212	0.040	0.00100
0.65	0.0203	0.031	0.00060
0.75	0.0198	0.024	0.00035
0.85	0.0189	0.018	0.00025
0.95	0.0174	0.016	0.00020

Then by making use of the extended Lagally Theorem (see Eq.24), the blade frequency force exerted on the spheroidal head in the fully-submerged case will be given by

$$\bar{F}_N = -4\pi\rho_f \frac{\partial}{\partial t} \iint_S \bar{r}\sigma e^{iN\Omega t} dS - 4\pi\rho_f \iint_S \bar{V}_p e^{iN\Omega t}\sigma_o \, dS \qquad (45)$$

where the first term represents the time-dependent and the second the convective term of the force, and

$\bar{r}$ = position vector in the direction of the desired force

$\bar{V}_p$ = propeller-induced velocity vector

σ = amplitude of the blade frequency source density

σ_o = amplitude of the source density arising from the presence of the hull in the free stream

S = the entire wetted surface

In applying the foregoing formula, it was found that the convective term is negligibly small and so the term involving the time derivation can be considered the sole contributor to the blade frequency hull force. The time-dependent force (blade frequency force) in the i-direction is given in the program by

$$\bar{F}_i = -i4\pi\rho_f NaU^2 r_o^2 \iint_{S^*} \bar{r}_i^* \; \sigma^* dS^* \qquad (46)$$

and

$$C_{F_i} = \frac{\bar{F}_i}{\rho_f n^2 D^4} \qquad \text{where} \quad n = rps$$

and where all the "starred" quantities are nondimensionalized with respect to propeller radius r_o.

The theoretical results are given in the following Table 3 and the comparison with experiments is graphically exhibited in Figure 6. The graphical comparison shows agreement in magnitude of theoretical predictions with corresponding experimental measurements within 11%, and good agreement in phase angle θ_F. θ_F is generally defined as the reference blade position when the force on the body is maximum positive away from the propeller.

TABLE 3

CALCULATED BLADE FREQUENCY VERTICAL FORCE COEFFICIENT FOR PROPELLER 4118 LOCATED 16-IN AFT OF A SPHEROIDAL BODY WITH TIP CLEARANCE, c = 3.0 INCHES

Contributors	F_y, Vertical Force, lb		$C_F = \dfrac{F_y}{\rho_f n^2 D^4}, \times 10^3$	θ_F = Phase Angle (Mechanical) in degrees with respect to Propeller Coordinates
	Real	Imaginary		
Thickness	1.263	-0.0133	2.820	-0.2°
Loading	-0.0920	-0.2078	0.507	-37.96°
Loading + Thickness	1.171	-0.2211	2.662	-3.56°

In this particular case with the experiments conducted with the propeller located on the portside of the spheroidal body, the measured and theoretically defined phase angles coincide.

It is to be noted that the contribution due to blade thickness dominates the force amplitude. This was also found by Breslin[14] who calculated the forces and moments on infinitely long cylinders.

CASE 2 — The Series 60, $0.6C_B$, hull model (V-stern) is similarly subdivided into quadrilaterals. There are 202 in all with the hull reflection in the waterplane included. In some of the quadrilaterals the propeller-induced velocities are neglected as being small. In fact, 96 of the quadrilaterals located at the forward part of the hull and its reflection have thus been deactivated (i.e., propeller-induced velocities are taken to be zero).

Particulars of the Propeller NSRDC 3379 are given in Table 4, and other characteristics are given in Table 5; the harmonic content of the wake behind the Series 60, $0.6C_B$ hull with V-shaped sections, is presented in Table 6.

TABLE 4

PARTICULARS OF PROPELLER 3379

Propeller Designation	NSRDC 3379
Model Designation	Series 60, C_B=0.6, V-form
Number of Blades	4
EAR	0.471
P/D at 0.7 radius	1.02
Diameter, D , ft	0.4167
RPM, 60n	787.5
Model Speed, U , ft/sec	4.56
J = U/nD	0.834

TABLE 5

CHARACTERISTICS OF PROPELLER 3379

z/z_o	Maximum camber/chord m_x/c	Maximum thickness/chord t_o/c	σ = skewness in radians
0.25	0.0254	0.1651	0.023
0.35	0.0254	0.1303	0.060
0.45	0.0263	0.1044	0.105
0.55	0.0265	0.0846	0.143
0.65	0.0257	0.0680	0.160
0.75	0.0240	0.0543	0.190
0.85	0.0207	0.0435	0.232
0.95	0.0174	0.0334	0.275

TABLE 6

HARMONIC CONTENT OF THE WAKE[*] OF A SERIES 60, 0.6 C_B MODEL WITH V-FORM SECTIONS

a) Longitudinal Velocity Components

Radius	a_o	a_1	a_2	a_3	a_4	a_5	b_q
0.25	0.522	-0.093	-0.130	0.013	0	-0.005	0
0.35	0.640	-0.110	-0.190	0.027	-0.047	0.019	0
0.45	0.736	-0.104	-0.220	0.023	-0.075	0.027	0
0.55	0.791	-0.142	-0.192	-0.012	-0.080	0.020	0
0.65	0.813	-0.152	-0.165	-0.040	-0.071	0.008	0
0.75	0.818	-0.158	-0.147	-0.050	-0.057	-0.002	0
0.85	0.828	-0.162	-0.133	-0.057	-0.046	-0.012	0
0.95	0.845	-0.172	-0.122	-0.062	-0.037	-0.018	0

b) Tangential Velocity Components

Radius	A_q	B_1	B_2	B_3	B_4	B_5
0.25	0	-0.040	-0.040	0.037	-0.020	0
0.35	0	-0.093	-0.035	0.030	-0.019	0.010
0.45	0	-0.128	-0.033	0.019	-0.017	0.013
0.55	0	-0.133	-0.034	0.005	-0.014	0.010
0.65	0	-0.130	-0.036	-0.007	-0.009	0.005
0.75	0	-0.130	-0.038	-0.016	-0.008	-0.002
0.85	0	-0.128	-0.040	-0.020	-0.007	-0.006
0.95	0	-0.125	-0.041	-0.022	-0.007	-0.009

where

[*]Grant, J.W. and Lin, A.C., "The Effects of Variations of Several Parameters on the Wake in Way of the Propeller Plane for Series 60-0.60 C_B Models" Naval Ship Res. and Dev. Center Rpt. No.3024, June 1969.

$$\text{Longitudinal Velocity } V_X/U = a_o + \sum_{q=1}^{\infty} [a_q \cos q\theta + b_q \sin q\theta]$$

$$\text{Tangential Velocity } V_T/U = A_o + \sum_{q=1}^{\infty} [A_q \cos q\theta + B_q \sin q\theta]$$

Utilizing the extended Lagally Theorem over the double-hull body, the vertical component of the blade frequency force has been calculated as before, demonstrating again that the convective term is small. The theoretical results are given in Table 7.

TABLE 7

CALCULATED BLADE FREQUENCY VERTICAL FORCE COEFFICIENT
ON A SERIES 60, 0.6 C_B HULL (V-FORM) WITH THE 4-BLADED PROPELLER 3379
AT AXIAL CLEARANCE, x = 0.25D

Contributors	F_y=Vertical Force, $\times 10^2$, lb		Coefficient $C_F = \dfrac{F_y}{\rho_f n^2 D^4}$, $\times 10^4$	θ_F=Phase Angle (Mechanical) in degrees with respect to	
	Real	Imaginary		Body Coordinates	Propeller Coordinates
Thickness	0.9152	-0.2631	9.468	-4.01	41
Loading	1.8798	-1.4821	23.80	-9.56	35.44
Loading + Thickness]*	2.7950	-1.7452	32.74	-8.0	37.02
Bearing Force**	-0.392	-2.555	25.705	-	65.30
Net Force***	-3.187	-0.8098	32.886	-	48.52

*From Hess-Smith code with (+) vertical axis downwards.

**From DL Propeller Blade Pressure Distribution Program (PPEXACT) with (+) vertical axis upwards.

***Referred to Propeller coordinate axis with (+) vertical axis upwards.

NOTE: θ_F is physically interpreted as being the blade position when the force on the body is a positive maximum away from the propeller.

A barogram of the individual contributions to the hull surface force from blade thickness and blade loadings at harmonics of order 0,1,2,3,4 and 5, is shown in Figure 7, with, in addition, a comparison of the net vertical force coefficient (i.e., sum of total surface force and the corresponding bearing force) with the results of experiments conducted by the late Professor F.M. Lewis.[13]

It is seen that there is a difference between predictions and measurements of approximately 25%. In contrast, for the spheroidal body, the predictions are approximately 10% lower than the measurements. These differences can be attributed to several factors but are mainly due to the fact that

comparison with Lewis' data is not strictly valid since measurements of
the force include a combination of a force and a couple, whereas the
result of these calculations presents the value of the vertical force
only. Therefore, a one-to-one comparison cannot, in principle, be made.
Another possible source of uncertainty is the fact that the results
have not yet converged since, when reducing the mesh size and increasing
the number of quadrilaterals, the resulting force keeps changing value.
Furthermore, it is also possible for the existing differences to be
attributed to a certain degree to the fact the "complete" interaction
problem of the propeller and hull has not been taken into account. The
"complete" interaction problem involves the simultaneous mutual effect
of one surface on the other carried out in a "ping-pong" fashion until
stable values of hydrodynamic loadings and forces on both surfaces (pro-
peller and hull) are established. This process has been incorporated in
DL propeller-rudder and propeller-duct programs. The "feedback" of the
rudder to the propeller was found to be small.

The computing time in the present approach is relatively high for
practical use, a fact which excludes the possibility of any improvement
of the scheme by reducing the mesh size and increasing the number of
quadrilaterals. A different procedure, developed under MARAD support,
(mentioned in the INTRODUCTION) creates the hull surface by a doublet
distribution. This method is much more effective in achieving accuracy
and reduces the computing time considerably compared to that incurred
at present by using a hull source density distribution. The results of
this new approach are also exhibited in Figure 6 and 7. The "differences"
for the spheroidal head have been reduced to 2%, and for the Series 60
model, to 10%.

CONCLUSIONS

A method based on rational mechanics is elucidated for predicting the hydrodynamic forces and moments acting on a hull of arbitrary geometry as a reaction to the propeller-induced velocity field. A distribution of sources generates the hull in both uniform and propeller-induced flows, in the presence or absence of a free surface. A computer program, based on this procedure and adapted to the CDC 7600 or Cyber 176 digital computer, provides the strengths of the sources from which all the vertical components of the blade-frequency propeller-induced hull forces can be found. Evaluation has been limited to the vertical force.

The program is very general, i.e., it is applicable to any propeller and hull of arbitrary form. However, it requires that the hull be sub-divided into a large number of quadrilaterals in order to obtain accurate, reliable results. Since the propeller-induced velocity field is generally spatially oscillatory in character, the dimensions of each quadrilateral must be such as to fit at least four of them into one cycle of oscillation. In addition, the normal velocity to each quadrilateral requires the evaluation of three velocity components for all possible combinations of frequencies of loading with those of the propagation functions. This part of the program is the most time-consuming (taking 80-85% of the computer time) and demands great attention to secure convergence. The excessive number of quadrilaterals, coupled with complications arising from the propeller-induced velocity, makes this particular numerical method expensive and rather impractical.

A new procedure has been developed under subsequent MARAD support in which the hull is generated by a doublet distribution. The doublet strengths are evaluated by means of an integral equation similar to that used in the present study, but which requires, instead of the three normal components of the propeller-induced velocity at each quadrilateral, the propeller-induced velocity potential (a scalar function) at the null point at each inner side of the panel. In this way, the time for computation is reduced to almost half that incurred at present. The results of

this new procedure (exhibited in Figures 6 and 7) show much reduced discrepancies when compared with the experimental results. The "differences" for the Series 60 model have been reduced from 27% to 10% and for the spheroidal body from 11% to 2%. It is to be kept in mind, of course, that the force measurements include a combination of a force and a couple, whereas the results of calculations present values of vertical force only.

This method of doublet distribution is being employed for a series of surface ship cases tested by the late Professor Emeritus F.M. Lewis at MIT in a new study, which will be reported in the near future.

ACKNOWLEDGMENTS

REFERENCES

1. Breslin, J.P. and Eng, K., "A Method for Computing Propeller-Induced Vibratory Forces on Ships," First Conference on Ship Vibration, Stevens Institute of Technology, 25 January 1965.

2. Hess, J.L. and Smith, A. M., "Calculation of Non-Lifting Potential Flow About Arbitrary Three-Dimensional Bodies," Douglas Aircraft Division, Report No.E.S.40622, 15 March 1962.

3. Breslin, J.P. and Tsakonas, S., "The Blade-Frequency Velocity Field Near an Operating Marine Propeller Due to Loading and Thickness Effects," Proceedings of Sixth Midwestern Conference of Fluid Mechanics, 1959.

4. Vorus, W.S., "A Method for Analyzing the Propeller-Induced Vibratory Forces Acting on the Surface of a Ship Stern," Trans. SNAME, Nov. 1974.

5. Tsakonas, S., Jacobs, W.R., and Ali, M.R., "Propeller Blade Pressure Distribution Due to Loading and Thickness Effects," Report SIT-DL-76-1869, April 1976, J. Ship Research, Vol.23, No.2, June 1979.

6. Tsakonas, S., Jacobs, W.R., and Ali, M.R., "Documentation of a Computer Program for the Pressure Distribution, Forces and Moments on Ship Propellers in Hull Wakes," Report SIT-DL-76-1863.

7. Tsakonas, S. and Jacobs, W.R., "Steady and Time-Dependent Propeller Blade Loading and Stress Analysis," Proceedings, Propellers 75 Symposium, SNAME, July 1975.

8. Jacobs, W.R. and Tsakonas, S., "Propeller Loading Induced Velocity Field by Means of the Unsteady Lifting Surface Theory," J. Ship Research, Vol.17, No.3, September 1973.

9. Jacobs, W.R. and Tsakonas, S., "Propeller-Induced Velocity Field Due to Thickness and Loading Effects," J. Ship Research, Vol.19, No.1, March 1975.

10. Kellogg, O.D., Foundations of Potential Theory, Dover Publications, Inc., 1929.

11. Cox, B.D., Vorus, W.S., Breslin, J.P., and Rood, E.P., "Recent Theoretical and Experimental Developments in the Prediction of Propeller-Induced Vibratory Forces on Nearby Boundaries," presented at 12th Symposium on Nav. Hydrodynamics, Off. of Naval Res., Wash., DC, June 1978.

12. Jacobs, W.R., Valentine, D.T., and Ali, M.R., "Documentation of a Computer Program for the Velocity Field Induced by a Marine Propeller — User's Manual," Report SIT-DL-78-9-2042.

13. Lewis, F.M., "Propeller Vibration Forces in Single-Screw Ships," Paper presented at the SNAME Annual Meeting, New York, Nov.12-14, 1969.

14. Breslin, J.P., "Review and Extension of Theory for Near-Field Propeller-Induced Vibratory Effects," Proc. of Fourth Symposium on Naval Hydrodynamics Hydroelasticity, ONR, August 1962.

S = Hull Surface

S$_1$ = Water Plane
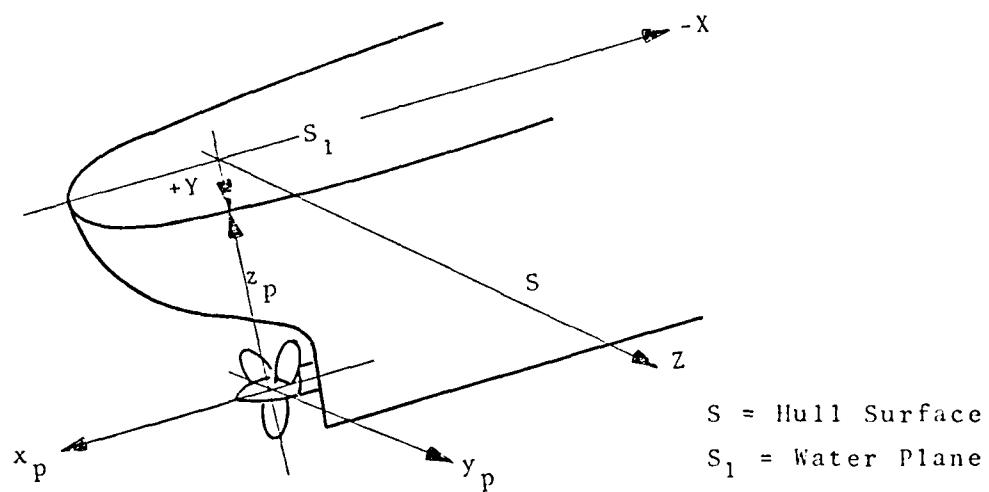
FIGURE 1.   PROPELLER-SERIES 60 HULL ARRANGEMENT WITH
COORDINATE AXES WITH RESPECT TO PROPELLER
AND TO HULL

R-1979

AFT VIEW IN PROPELLER PLANE

PLAN VIEW
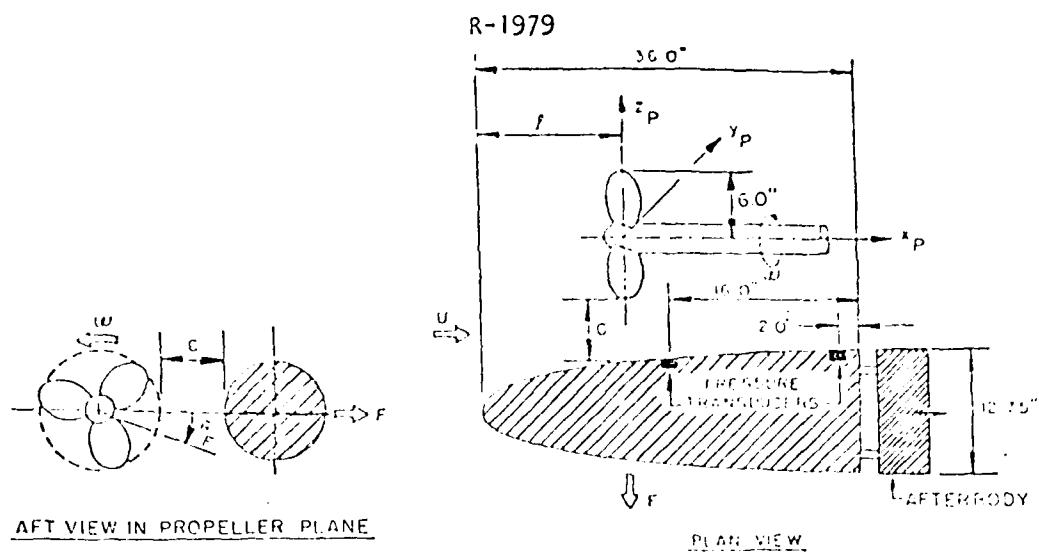
FIGURE 2.   PROPELLER-SPHEROIDAL HEAD ARRANGEMENTS
             -COORDINATE SYSTEM
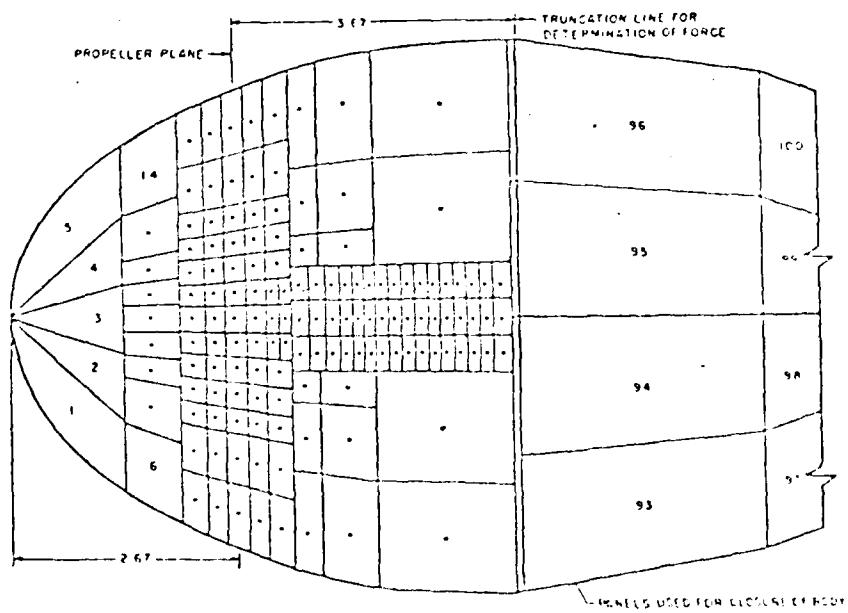

FIGURE 3.   SCHEMATIC OF EXPANDED SURFACE OF DTNSRDC
             ELLIPSOIDAL TEST BODY DIVIDED INTO 154
             SOURCE PANELS (DIMENSIONS IN MULTIPLES
   OF PROPELLER RADIUS)
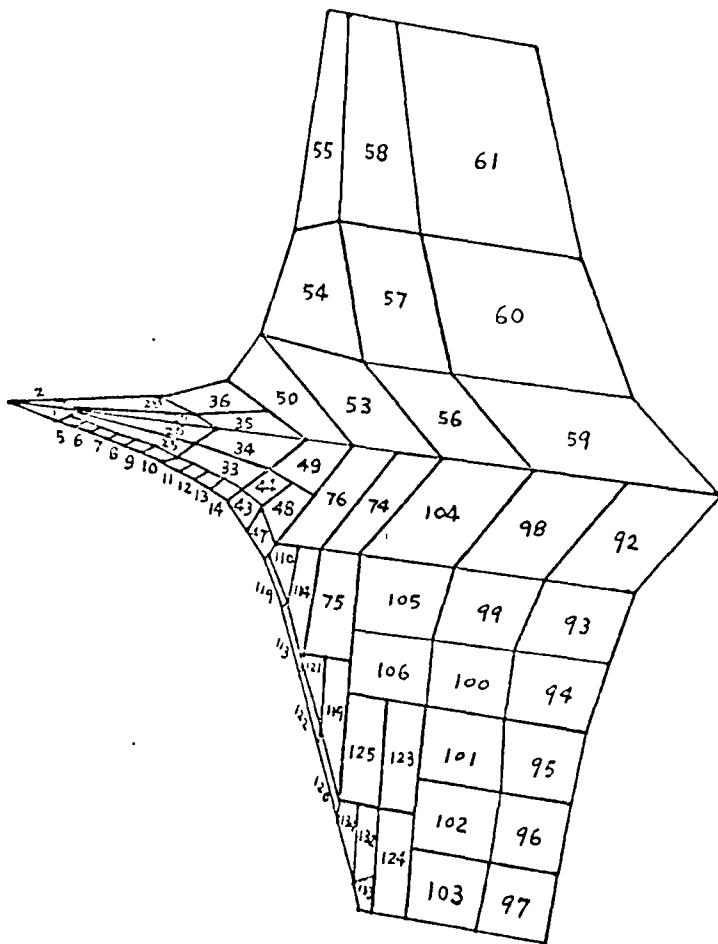
FIGURE 4a.   SOURCE PANEL DISTRIBUTION ON "DOUBLE" HULL
(SERIES 60, C_B = 0.6, V-SECTIONS AFT).   ENTIRE
HULL PLUS REFLECTION IN AN INFINITE FLUID,
STARBOARD SIDE.
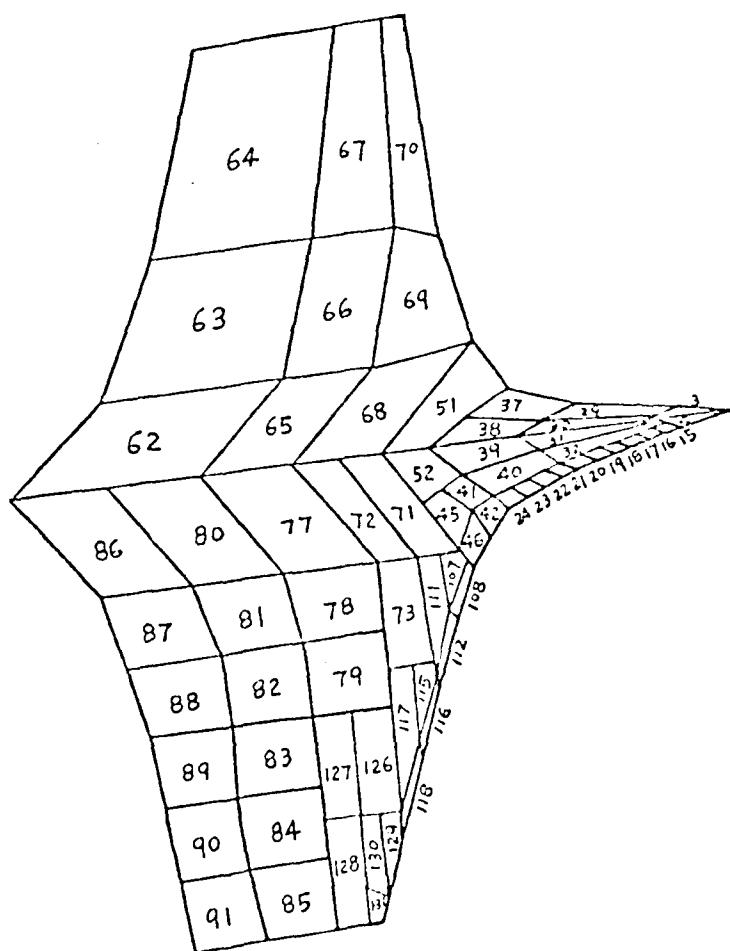
FIGURE 4b.   SOURCE PANEL DISTRIBUTION ON "DOUBLE" HULL
(SERIES 60, C_B = 0.6, V-SECTIONS AFT).   ENTIRE
HULL PLUS REFLECTION IN AN INFINITE FLUID,
PORT SIDE.
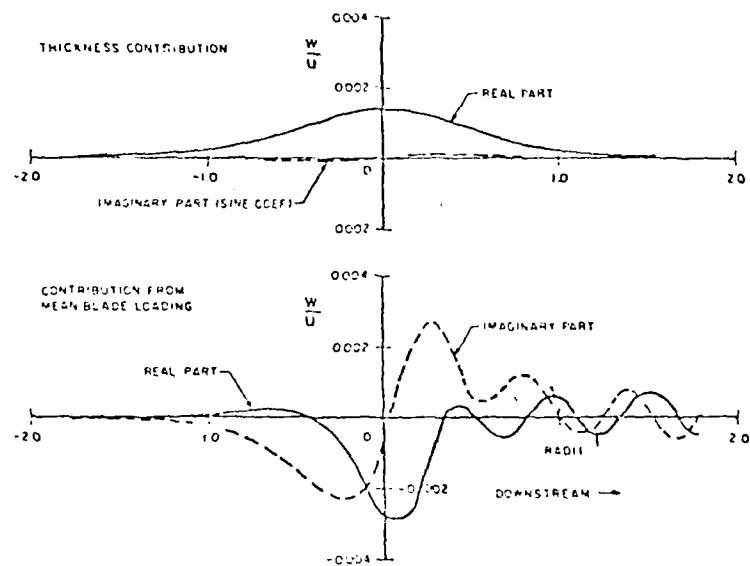
FIGURE 5.   VARIATION OF BLADE FREQUENCY VERTICAL
             VELOCITIES INDUCED BY 3-BLADED DTNSRDC
             PROPELLER 4118 AT $r=1.5R_o$ AND $\varphi=0$
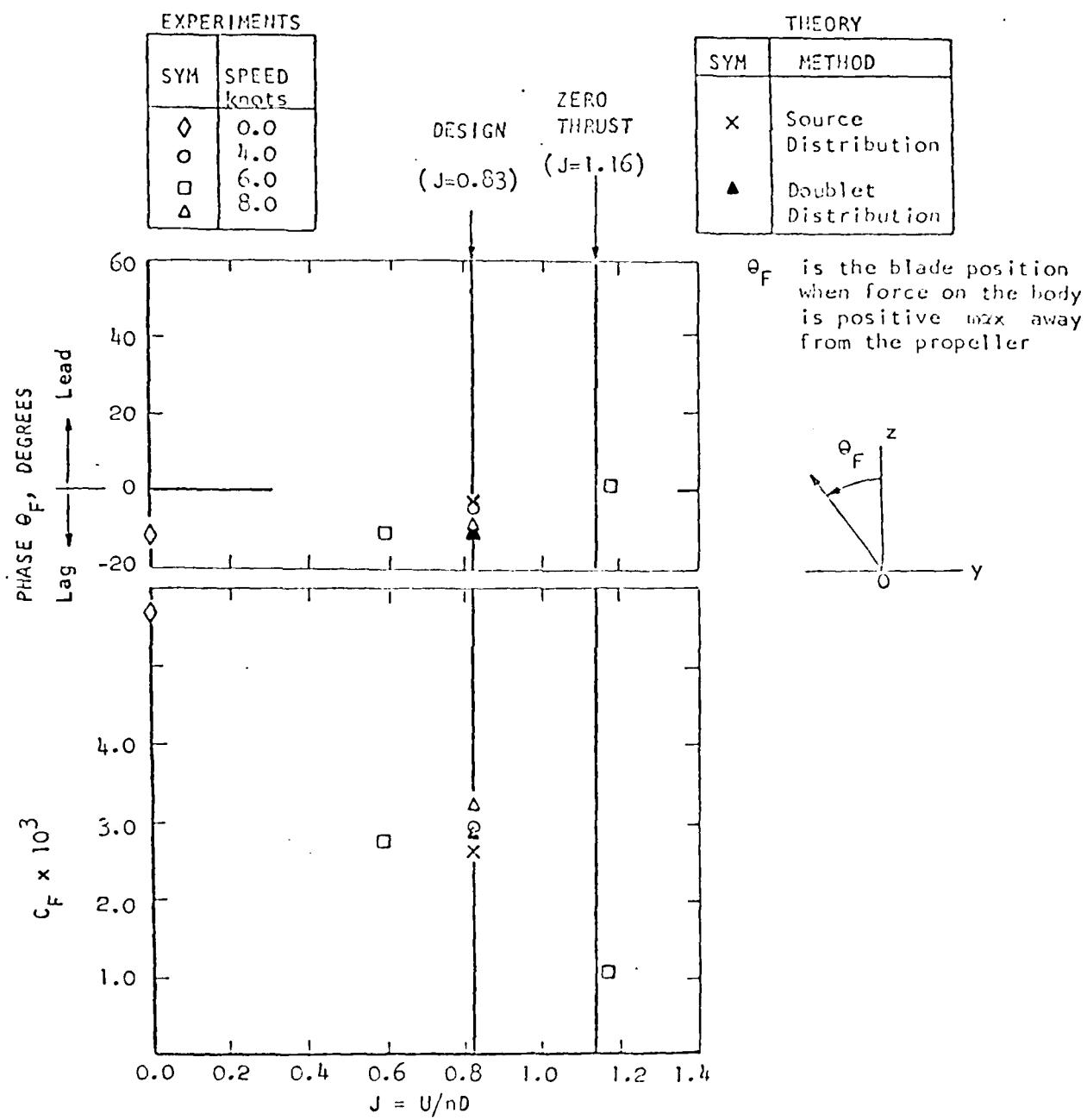
FIGURE 6. CALCULATED AND MEASURED BLADE FREQUENCY FORCE FOR PROPELLER LOCATED AT 1 = 16.0 IN. WITH TIP CLEARANCE C = 3.0 IN.
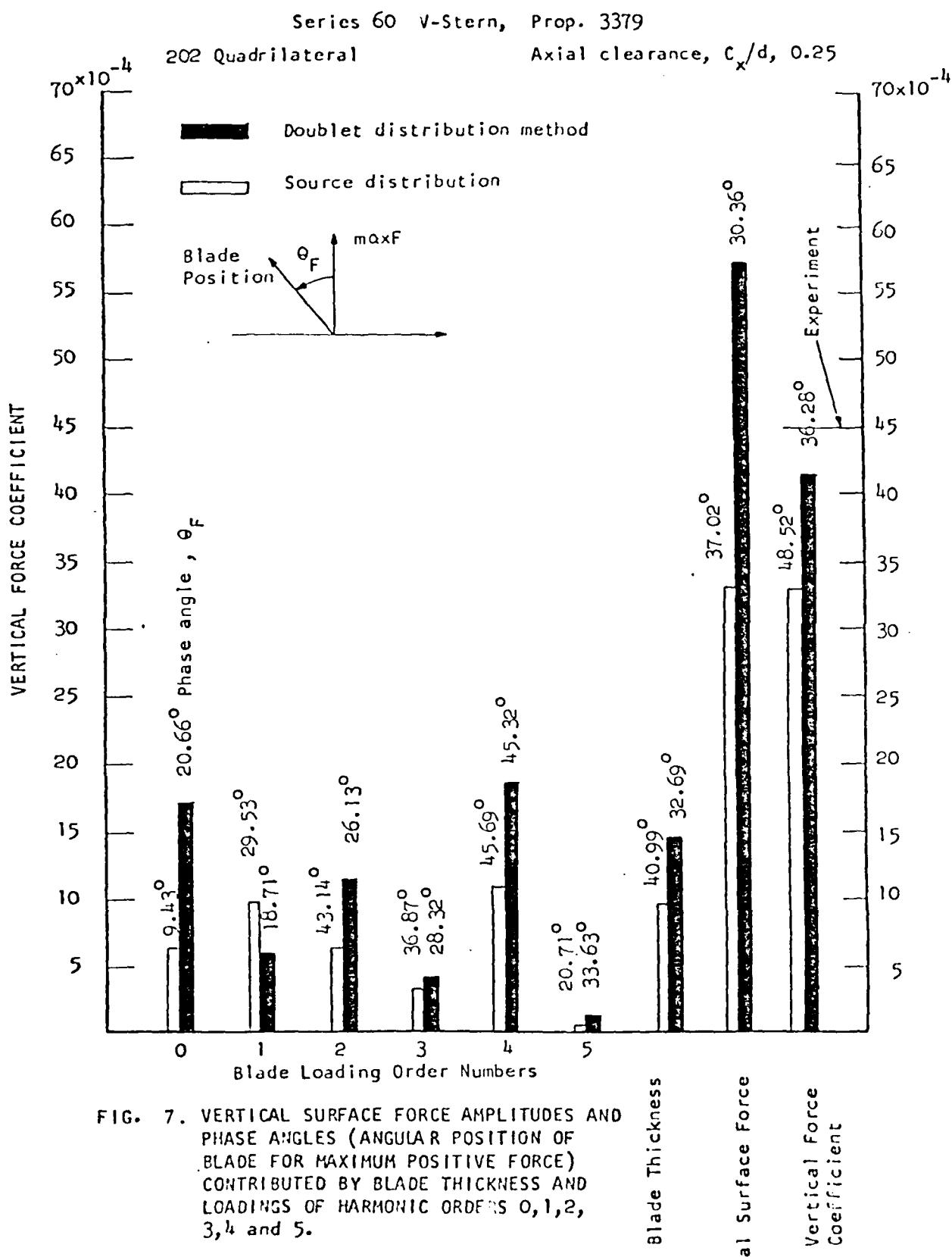
FIG. 7. VERTICAL SURFACE FORCE AMPLITUDES AND PHASE ANGLES (ANGULAR POSITION OF BLADE FOR MAXIMUM POSITIVE FORCE) CONTRIBUTED BY BLADE THICKNESS AND LOADINGS OF HARMONIC ORDERS 0,1,2, 3,4 and 5.

APPENDIX

COMPUTER PROGRAM

The program based on the foregoing analysis is written in FORTRAN IV language and checked out and run on control data high-speed digital computers (CDC-6600, CDC-7600, and Cyber 176). The calculations on CDC-6600 and 7600 computers were run with KRONOS and SCOPE operating systems, respectively, and then on Cyber 176 by making use of the NOSBE system.

The final program of the "Propeller-Hull Interaction" problem coded as "PIHF" is the result of a combination of the "Hess-Smith" program (H-S code) with the propeller-induced velocity field program "VFDTL" and the subroutine designated "FORCE" which implements the extended "Lagally" Theorem. Sketch #1 exhibits the Flow Diagram connecting the various subprograms to generate the final form of the "PIHF" code.

Although the program is very lengthy, it can be run in its complete form (i.e., H-S code + VFDTL + FORCE). It is advisable, however, to execute the program in stages for better control of the input from one subprogram to another and for keeping track of the accuracy of the results at each stage.

Initially the "PPEXACT" program is executed furnishing the propeller loading information at all shaft frequencies which will be recorded on a magnetic-tape and utilized at the proper time in the "PIHF" code. Then the part of the "Hess-Smith" program dealing with the geometry of the hull form and with the quadrilaterals into which the hull surface is subdivided, will be executed, furnishing information about the direction cosines of the outward directed normal on each quadrilateral, the coordinates at the "null-points," and the corresponding area. The null points which are expressed with respect to hull coordinate axes will be transferred to the propeller axes and saved.

At this stage the propeller-induced velocity field will be calculated through the "VFDTL" code at the null-points previously determined. This step is the most time-consuming one and should be done carefully by plotting the results and keeping track of the convergence.

These propeller-induced velocities will be utilized in the final part of the "Hess-Smith" program which deals with the solution of the integral equation. The solution determines the strengths, σ , of the source distribution and these, in turn, will be utilized in the "FORCE" coding to determine the hydrodynamic forces and moments exerted on the hull, in reacting to the propeller action. The program, however, provides meaningful results for the vertical component only. The presence of the free surface generates a "momentum flux" through the waterplane area. The vertical component of the "momentum flux" does not affect the vertical component of the hydrodynamic force (see the Lagally Theorem) whereas the axial and transverse components are influenced by the momentum flux.

Calculations were performed, as mentioned before, for the "spheroidal head" and for a surface ship of one of the Series 60, C_B = 0.60, models. The table below shows approximate computational periods running the program with the NOSBE operating system on the Cyber 176 high-speed digital computer:

TABLE

COMPUTING TIME IN SYSTEM RESOURCE UNITS, SRU, ON CYBER 176

AND CPU (seconds)

1) Spheroidal body with 3-bladed propeller DTNSRDC 4118 operating in a uniform inflow. Body is subdivided into 154 quadrilaterals.

| Program	CPU-Time(sec)[*]	SRU
PPEXACT (Q=0)	11.5	41
PIHF { H-S (basic)	4	15
VFDTL	206	738
H-S & Force	15	54
	236.5 (3.94 min.)	848

2) Series 60, C_B=0.60, equipped with 5-bladed propeller 3379. Hull surface is subdivided into 202 quadrilaterals with only 134 quadrilaterals activated.

PROGRAM	CPU-Time(sec)[*]	SRU
PPEXACT	66	236
PIHF { H-S (basic)	5.5	19
VFDTL(Q=0,1,..,6)	528	1893
H-S & Force	15	54
	614.5 (10.24 min.)	2202

[*]If the CDC-7600 or CDC-6600 computers are used operating under KRONOS and SCOPE systems, respectively, then the times should be increased approximately by a factor of 1.7 and 8.2, respectively.

SKETCH 1

FLOW DIAGRAM FOR "PIHF" PROGRAM
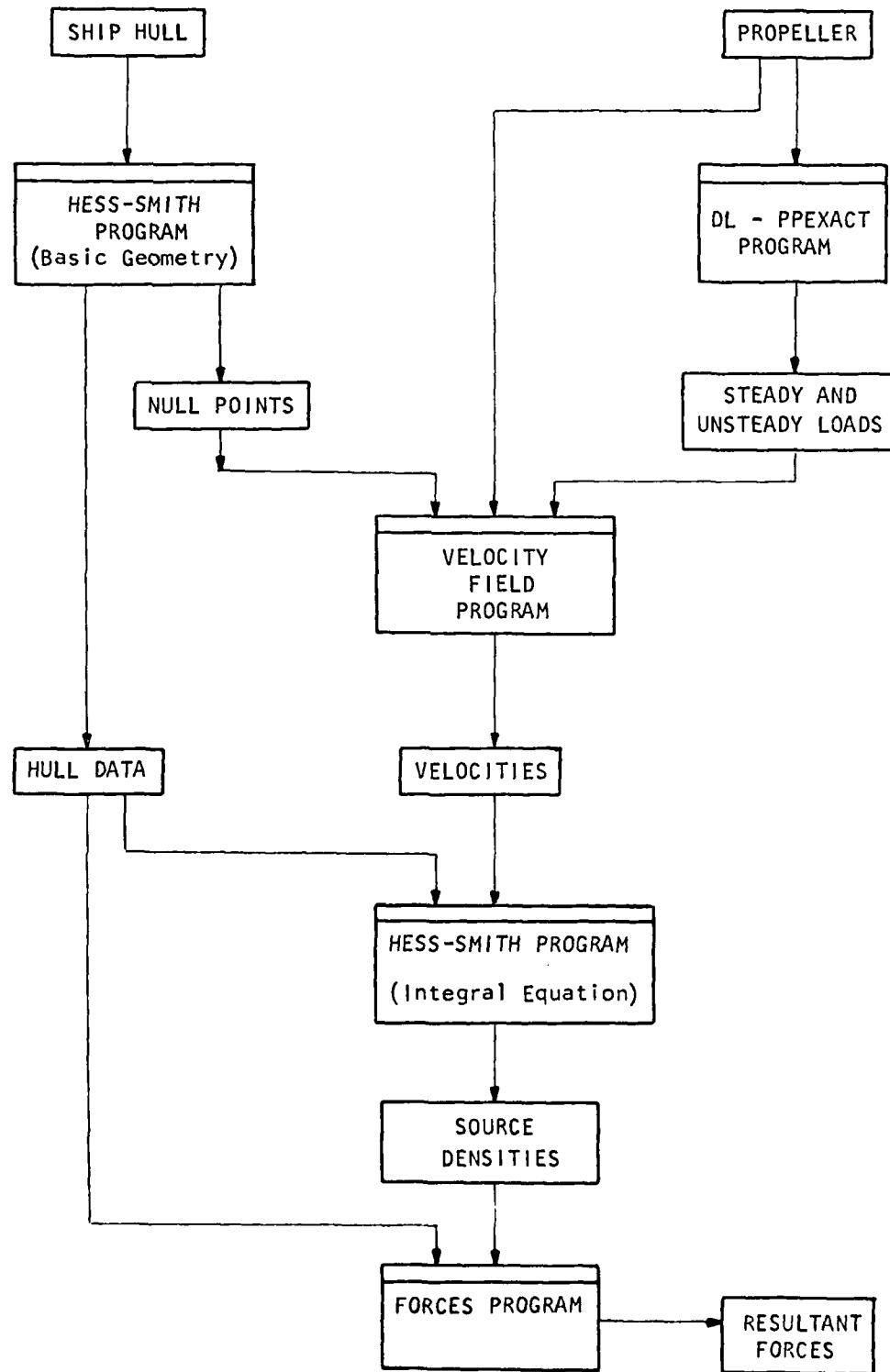
DISTRIBUTION LIST
(Contract N00014-76-C-0862)

10 Commander
    DAVID W. TAYLOR NAVAL SHIP
      R&D CENTER (Code 1543)
    Bethesda, MD 20084

    Officer-in-Charge
    Annapolis Laboratory
    DAVID W. TAYLOR NAVAL SHIP
      R&D CENTER (Code 522.3)
    Annapolis, MD 21402

10 Commander
    NAVAL SEA SYSTEMS COMMAND
    Washington, DC 20362
    Attn: SEA 32R
           312
           3213
           05H
           05R11
           52
           521
           524
           52P
           99612

12 Director
    DEFENSE TECHNICAL INFORMATION CENTER
    5010 Duke Street
    Alexandria, VA 22314

    OFFICE OF NAVAL RESEARCH
    800 N. Quincy Street (Code 438)
    Arlington, VA 22217

    OFFICE OF NAVAL RESEARCH
    Branch Office (493)
    536 S. Clark Street
    Chicago, IL 60605

    Chief Scientist
    OFFICE OF NAVAL RESEARCH
    Branch Office
    1030 E. Green Street
    Pasadena, CA 91106

    OFFICE OF NAVAL RESEARCH
    Resident Representative
    715 Broadway (5th Floor)
    New York, NY 10003

Director (Code 2027)
NAVAL RESEARCH LABORATORY
Washington, DC 20390

Commander
NAVAL FACILITIES ENGINEERING
  COMMAND (Code 032C)
Washington, DC 20390

LIBRARY OF CONGRESS
Science and Technology Division
Washington, DC 20540

Commander (ADL)
NAVAL AIR DEVELOPMENT CENTER
Warminster, PA 18974

NAVAL UNDERWATER WEAPONS RESEARCH
  & ENGINEERING STATION (LIBRARY)
Newport, RI 02840

Commanding Officer (L31)
NAVAL CIVIL ENGINEER'G LABORATORY
Port Hueneme, CA 93043

4 Commander
    NAVAL OCEAN SYSTEMS CENTER
    San Diego, CA 92152
    Attn: Dr. A. Fabula (4007)
          Dr. J. Hoyt (2501)
          Dr. M. Reichman (6342)
          Library

Library
NAVAL UNDERWATER SYSTEMS CENTER
Newport, RI 02840

Research Center Library
WATERWAYS EXPERIMENT STATION
CORPS OF ENGINEERS
P.O. Box 631
Vicksburg, MS 39180

CHARLESTON NAVAL SHIPYARD
Technical Library
Naval Base
Charleston, SC 29408

OFFICE OF NAVAL RESEARCH
San Francisco Area Office
760 Market Street (Room 447)
San Francisco, CA 94102

DISTRIBUTION LIST
(Contract N00014-76-C-0862)

NORFOLK NAVAL SHIPYARD
Technical Library
Portsmouth, VA 23709

PORTSMOUTH NAVAL SHIPYARD
Technical Library
Portsmouth,NH 03801

PUGET SOUND NAVAL SHIPYARD
Engineering Library
Bremerton, WA 98314

LONG BEACH NAVAL SHIPYARD
Technical Library (246L)
Long Beach, CA 90801

MARE ISLAND NAVAL SHIPYARD
Shipyard Technical Library (202.3)
Vallejo, CA 94592

Assistant Chief Design Engineer
 for Naval Architecture (250)
MARE ISLAND NAVAL SHIPYARD
Vallejo, CA 94592

2 U.S. NAVAL ACADEMY
Annapolis, MD 21402
Attn: Technical Library
       Dr. S.A. Elder

NAVAL POSTGRADUATE SCHOOL
Library (2124)
Monterey, CA 93940

Study Center
National Maritime Research Center
U.S. MERCHANT MARINE ACADEMY
Kings Point
Long Island, NY 11024

THE PENNSYLVANIA STATE UNIVERSITY
Applied Research Lab (Library)
P.O. Box 30
State College, PA 16801

Dr. B. Parkin, Director
Garfield Thomas Water Tunnel
APPLIED RESEARCH LABORATORY
P.O. Box 30
State College, PA 16801

BETHLEHEM STEEL CORPORATION
25 Broadway
New York, NY 10004
Attn: Library - Shipbuilding

CAMBRIDGE ACOUSTICAL ASSOC., INC.
54 Rindge Avenue Extension
Cambridge, MA 02140

R&D Manager
Electric Boat Division
GENERAL DYNAMICS CORPORATION
Groton, CT 06340

GIBBS & COX, INC.
Technical Information Control
21 West Street
New York, NY 10006

2 HYDRONAUTICS, INC.
Pindell School Road
Laurel, MD 20810
Attn: Library
       Mr. J. Otto Scherer

2 MCDONNELL DOUGLAS AIRCRAFT COMPANY
3855 Lakewood Boulevard
Long Beach, CA 90801
Attn: Dr. T. Cebeci
       Mr. J. Hess

NEWPORT NEWS SHIPBUILDING AND
 DRYDOCK COMPANY (TECH.LIBRARY)
4101 Washington Avenue
Newport News, VA 23607

Mr. S. Spangler
NIELSEN ENGINEERING & RESEARCH,INC.
510 Clyde Avenue
Mountain View, CA 94043

SOCIETY OF NAVAL ARCHITECTS AND
 MARINE ENGINEERS (TECH. LIBRARY)
One World Trade Center,Suite 1369
New York, NY 10048

Chief Naval Architect
SUN SHIPBUILDING & DRY DOCK COMPANY
Chester, PA 19000

DISTRIBUTION LIST
(Contract N00014-76-C-0862)

Library
BOLT, BERANEK & NEWMAN
50 Moulton Street
Cambridge, MA 02138

2 SOUTHWEST RESEARCH INSTITUTE
P.O. Drawer 28510
San Antonio, TX 78284
Attn: Applied Mechanics Review
       Dr. H. Abramson

TRACOR, INC.
6500 Tracor Lane
Austin, TX 78721

Mr. Robert Taggart
9411 Lee Highway, Suite P
Fairfax, VA 22031

Ocean Engineering Department
WOODS HOLE OCEANOGRAPHIC, INC.
Woods Hole, MA 02543

WORCESTER POLYTECHNIC INSTITUTE
Alden Research Lab (Tech. Library)
Worcester, MA 01609

Applied Physics Laboratory
UNIVERSITY OF WASHINGTON
Technical Library
1013 N.E. 40th Street
Seattle, WA 98105

4 UNIVERSITY OF CALIFORNIA
Naval Architecture Department
Berkeley, CA 94720
Attn: Prof. W. Webster
       Prof. J. Paulling
       Prof. J. Wehausen
       Library

3 CALIFORNIA INSTITUTE OF TECHNOLOGY
Pasadena, CA 91109
Attn: Dr. T.Y. Wu
       Dr. A.J. Acosta
       Library

Engineering Research Center
   Reading Room
COLORADO STATE UNIVERSITY
Foothills Campus
Fort Collins, CO 80521

Library
STANFORD RESEARCH INSTITUTE
Menlo Park, CA 94025

2 FLORIDA ATLANTIC UNIVERSITY
Ocean Engineering Department
Boca Raton, FL 33432
Attn: Technical Library
       Dr. S. Dunne

Gordon McKay Library
HARVARD UNIVERSITY
Pierce Hall
Cambridge, MA 02138

Library
Department of Ocean Engineering
UNIVERSITY OF HAWAII
2565 The Mall
Honolulu, HI 96822

2 Institute of Hydraulic Research
THE UNIVERSITY OF IOWA
Iowa City, IA 52240
Attn: Library
       Dr. L. Landweber

Prof. D. Nesmith
KANSAS STATE UNIVERSITY
Engineering Experiment Station
Seaton Hall
Manhattan, KS 66502

UNIVERSITY OF KANSAS
Chm Civil Engineering
   Department Library
Lawrence, KS 60644

Fritz Engr. Laboratory Library
Department of Civil Engineering
LEHIGH UNIVERSITY
Bethlehem, PA 18015

3 Department of Ocean Engineering
MASSACHUSETTS INST. OF TECHNOLOGY
Cambridge, MA 02139
Attn: Prof. P. Leehey
       Prof. J. Newman
       Prof. J. Kerwin

SPERRY SYSTEMS MANAGEMENT DIVISION
Sperry Rand Corporation (Library)
Great Neck, NY 11020

DISTRIBUTION LIST
(Contract N00014-76-C-0862)

MASSACHUSETTS INST. OF TECHNOLOGY
Engineering Technical Reports
Room 10-500
Cambridge, MA 02139

2 St. Anthony Falls Hydraulic Lab.
UNIVERSITY OF MINNESOTA
Mississippi River at 3rd Ave.,S.E.
Minneapolis, MN 55414
Attn: Dr. Roger Arndt
Library

3 Dept. of Naval Architecture and
Marine Engineering - North Campus
UNIVERSITY OF MICHIGAN
Ann Arbor, MI 48109
Attn: Library
Dr. T. Francis Ogilvie
Dr. W. Vorus

2 Davidson Laboratory
STEVENS INSTITUTE OF TECHNOLOGY
711 Hudson Street
Hoboken, NJ 07030
Attn: Library
Dr. J.P. Breslin

Applied Research Laboratory Library
UNIVERSITY OF TEXAS
P.O. Box 8029
Austin, TX 78712

Dr. Peter Fitzgerald, Manager
Naval Architecture & Structures
EXXON INTERNATIONAL
Tanker Research & Development
220 Park Avenue
Florham Park, NJ 07932

Mr. Merville E. Willis
SUN SHIPBUILDING & DRYDOCK COMPANY
Foot of Morton Avenue
Chester, PA.19013

25 MARITIME ADMINISTRATION
14th & E Streets, N.W.
Washington, DC 20230
Attn: M. Lasky (1)
R. Falls (1)
J. Nachtsheim (1)
F. Dashnaw (1)
F. Siebold (1)
Library (20)

2 STANFORD UNIVERSITY
Stanford, CA 94305
Attn: Engineering Library
Dr. R. Street

Library
WEBB INSTITUTE OF NAVAL
ARCHITECTURE
Crescent Beach Road
Glen Cove
Long Island, NY 11542

NATIONAL SCIENCE FOUNDATION
Engineering Division Library
1800 G Street, N.W.
Washington, DC 20550

Dr. Douglas E. Humphreys (794)
NAVAL COASTAL SYSTEMS LABORATORY
Panama City, FL 32401

Dr. Bruce D. Cox
HYDRODYNAMICS RESEARCH
ASSOCIATES, INC.
6000 Executive Boulevard
Room 308
Rockville, MD 20852

Mr. Everett Reed
LITTLETON RESEARCH & ENGR'G CORP.
95 Russell Street
Littleton, MA 01460